

Reference

NBS
Publi-
cations



A11106 259796

82-2478

Application of the Method of Characteristics to Predict Attenuation in Unsteady Partially Filled Pipe Flow

U.S. DEPARTMENT OF COMMERCE
National Bureau of Standards
Center for Building Technology
Washington, DC 20234

and

Drainage Research Group
Department of Building Technology
Brunel University
Uxbridge, U.K.

December 1981

Issued March 1982



QC

100

.U56

82-2478

1981

U.S. DEPARTMENT OF COMMERCE
NATIONAL BUREAU OF STANDARDS

NATIONAL BUREAU
OF STANDARDS
LIBRARY

MAY 17 1982

Not acc - Ry

QC100

. U56

no. 82-2478

1982

NBSIR 82-2478

**APPLICATION OF THE METHOD OF
CHARACTERISTICS TO PREDICT
ATTENUATION IN UNSTEADY PARTIALLY
FILLED PIPE FLOW**

Dr. J. A. Swaffield

U.S. DEPARTMENT OF COMMERCE
National Bureau of Standards
Center for Building Technology
Washington, DC 20234

and

Drainage Research Group
Department of Building Technology
Brunel University
Uxbridge, U.K.

December 1981

Issued March 1982

U.S. DEPARTMENT OF COMMERCE, Malcolm Baldrige, *Secretary*
NATIONAL BUREAU OF STANDARDS, Ernest Ambler, *Director*

PREFACE

This report is one of a group documenting National Bureau of Standards (NBS) research and analysis efforts in developing water conservation test methods, analysis, economics, and strategies for implementation and acceptance. This work is sponsored by the Department of Housing and Urban Development/Office of Policy Development and Research, Division of Energy Building Technology and Standards, under HUD Interagency Agreement H-48-78.

Report prepared by Dr. J. A. Swaffield, Senior Lecturer, Drainage Research Group, Department of Building Technology, Brunel University, Uxbridge, U.K., during a study leave period as a guest research worker at NBS/Stevens Institute of Technology.

ABSTRACT

The mechanism of flow attenuation in partially filled unsteady pipe flow is presented and shown to have relevance to the design of gravity drainage systems.

The equations defining unsteady flow in partially filled pipe are derived and shown to be capable of solution by means of the method of characteristics. This technique as a method of predicting flow depth, velocity and wave speed along a long drainage pipe at a range of pipe gradients, diameters and roughness coefficients was tested by means of numerical examples for a series of simulations run on a digital computer. Additionally, limited experimental verification of the analysis technique is presented for the supercritical flow response to a short duration inflow surge.

Generally the technique developed was found to be applicable to the design of drainage systems and further work is proposed to both extend the experimental verification and for the greater complexity of the multi-branched pipe system.

Key words: building drainage; computer model; surge attenuation; unsteady flow.

CONTENTS

	<u>Page</u>
Notation	vix
1. INTRODUCTION	1
2. FLOW ATTENUATION IN LONG PARTIALLY FILLED PIPE FLOW	3
3. DEVELOPMENT OF THE NUMERICAL SOLUTION	6
3.1 Summary of the Method of Characteristics Solution of the Equations Defining Unsteady Flow in Partially Filled Pipe Flow	6
3.2 Partially Filled Pipe Flow Regimes	7
3.3 Application of the Method of Characteristics Solution to Drainage Flow	11
3.3.1 Initial Steady Conditions Along the Pipe Length	12
3.3.2 Internal or Nodal Points	14
3.3.3 Entry Boundary Conditions, Supercritical Flow	14
3.3.4 Entry Boundary Conditions, Subcritical Flow	14
3.3.5 Exit Boundary Conditions, Supercritical Flow	15
3.3.6 Exit Boundary Conditions, Subcritical Flow	15
4. CALCULATION TECHNIQUES AND PRESENTATION OF RESULTS	16
4.1 Determination of Normal and Critical Depths	16
4.2 Numerical Integration for Surface Profiles	16
4.3 Choice of Time Step	17
4.4 Presentation of Results	17
5. DISCUSSION OF UNSTEADY FLOW SIMULATION RESULTS	19
5.1 Influence of Specified Time Interval Grid Size on Predicted Flow Parameters	19
5.2 Influence of Surge Duration on Partially Filled Pipe Flow Response	20
5.3 Influence of Pipe Slope, Diameter and Roughness on Predicted Variations in Flow Depth and Velocity	21

CONTENTS (Cont.)

	<u>Page</u>
5.4 Influence of Initial Steady Flow Value on Predicted Flow Attenuation	22
5.5 Estimate of Computer Run Time	23
6. EXPERIMENTAL VERIFICATION	24
7. CONCLUSIONS AND FURTHER WORK	26
8. REFERENCES	27
Figures	28
Appendix I Program TRANSCC	52
Appendix II Typical Output TRANSCC, Supercritical Flow Case	71

LIST OF FIGURES

	<u>Page</u>
1	Propagation of positive and negative surges in partially filled pipe flow 28
2	Surge attenuation as observed in drainage pipe flow 29
3	Application of momentum equation to unsteady flow in a general open channel 30
4	Modification to specified time interval grid for sub and supercritical flow regimes 31
5	Application of specified time interval grid to subcritical partially filled pipe flow with known entry and exit boundary equations 32
6	Relationship between flow specific energy and flow depth, illustrating the boundary between sub and supercritical flow regimes 33
7	Summary of pipe cross section and depth dependent parameter calculations 34
8	Basis of gradually varied flow depth prediction 35
9	Schematic representation of numerical integration to determine water surface profile 36
10	Influence of the choice of pipe section length on subcritical flow parameter predictions 37
11	Influence of the choice of pipe section length on supercritical flow parameter predictions 38
12	Depth of flow predictions for a surge introduced into subcritical flow 39
13	Depth of flow prediction for a surge introduced into supercritical flow 40
14	Comparison of surge response to a 2 s peak duration inflow at pipe gradients of 1/100 and 1/300 41
15	Comparison of surge response to a 2 s and 6 s peak flow duration inflow at a pipe gradient of 1/300 42

LIST OF FIGURES (Cont.)

	<u>Page</u>
16 Comparison of surge response to a 6 s peak inflow duration at pipe gradients of 1/100 and 1/300	43
17 Flow attenuation along a 30 m pipe, 0.1 m diameter at gradients 1/40, 1/100 and 1/300	44
18 Flow depth predictions along a 30 m pipe at 1/40, 1/100 and 1/300 gradients in response to a 1.27/s peak inflow surge	45
19 Continuation of figure 18	46
20 Peak flow rate predicted along a 30 m pipe for pipe gradients 1/40, 1/100, 1/300 and pipe diameters of 0.15, 0.1, and 0.075 m	47
21 Peak flow rate and depth predictions along a 15 m pipe, diameter 0.1 m illustrating the dependence on roughness coefficient	48
22 Effect of the initial steady flow on response to a 4.2 l/s peak surge	49
23 Summary of experimental test rig and associated inflow and depth recording instrumentation	50
24 Comparison of observed and predicted water depth vs. time profiles	51

NOTATION

A	Pipe flow cross section area, m^2
C^+ , C^-	Notation referring to the positive and negative characteristics
c	Wave speed, m/s
E	Specific energy = $h + V^2/2g$, m
F_r	Froude $N^\circ = V/\sqrt{gh}$
g	Acceleration due to gravity, m/sec^2
h	Flow depth, m
m	Hydraulic mean depth, m
N, n	N° of pipe length sections employed
P	Wetted channel perimeter, m
Q	Flow rate, l/s
S_0	Pipe slope
S	Slope of energy grade line, defined by Manning's Equation
T	Surface width of flow within partially filled channel, m
t	Time, sec
V	Local mean velocity, m/s
X1-4	Functions of h, V, c and S calculated at each base point at each time step
x	Distance, positive in initial flow direction, m
α	Pipe slope, $S_0 = \sin\alpha$
Δt	Time step, sec
Δx	Pipe section length, m
θ	$\Delta t/\Delta x$, sec/m; also subtended angle in figure 7
ρ	Fluid density, $gm\ sec^2/m^4$

NOTATIONS (Cont.)

τ_0 Wall to fluid shear stress, gm/m^2

Suffixes

A, B, C Calculated points in an x-t grid at time t

c Critical flow conditions

n Normal flow conditions

P Calculated points in an x-t grid at time $t + \Delta t$

R, S Interpolated points in an x-t grid at time t

U, D Upstream and downstream conditions relative to the solid boundary

1. INTRODUCTION

Observations of flow in long partially filled drainage pipes has shown that the shape of an input surge wave is materially altered during its passage along the system. In the absence of any downstream inflow the surge is observed to attenuate, that is the depth of water in the pipe decreases and the time taken for the surge to pass any station is seen to increase, indicating a reduced flow rate at any downstream time and distance coordinates.

This effect is of course well known and has been observed in large scale open channel flow and in flood routing studies. In the uniform channel case it is dependent on frictional effects, while the similar observations in flood routing are also dependent on the variable storage characteristics of the natural valleys followed by the flood.

In the design of drainage systems this flow attenuation can be of significant importance, particularly in the context of reduced water consumption. In simplifying some of the criteria commonly applied to drainage design it is possible to highlight two conflicting criteria that are affected by flow attenuation:

- (1) The prevention of pressure variations within a building's drainage pipework in order to avoid the diminution of appliance trap seals is a major design criterion. If the flow in a portion of the pipe system becomes full bore then positive air pressures are generated that can force odors past trap seals. Thus the maintenance of partially filled pipe flow is a major consideration and has led historically to conservative pipe sizing.
- (2) The removal of waste solids discharged into the drainage system is to a large extent dependent on the maintenance of flow depth behind the solid during its transportation. It will be seen that this criterion can be considered as being in possible opposition to the need to retain a clear air passage through the pipe network.

An accurate prediction technique for flow attenuation that was capable of dealing with both random inflows along the length of a drain pipe and a variable loading in terms of frequency of use of the appliances served by the system would be capable of effecting design decisions under both the criteria outlined above.

By definition therefore the technique would have to be a numerical solution based on relatively small time increments and capable of modelling the hydraulic properties of the system as well as being applicable in a general way to quite complex pipe networks.

The flow in the drainage system at any time may be generally described by the unsteady flow differential equations. Based on the application of the principles of momentum and flow continuity to an element of flow a pair of hyperbolic partial differential equations may be shown to describe the flow in terms of two independent variables, distance x and time t , and two dependent

variables, flow depth and velocity. These equations, that have been fully developed in an earlier report [1], may be solved numerically by performing two basic steps, first a combination of the equations to yield a pair of finite difference algebraic equations applicable along predetermined characteristics drawn in the x-t plane, and the solution of these equations with representative system boundary conditions.

This solution technique, known generally as the method of characteristics, meets the solution criteria set out above and indeed has been used extensively in the analysis of pressure surge in full bore complex pipe networks.

This report therefore presents the results of a series of computer simulations for partially filled flow attenuation in drainage sized pipes subject to typical prescribed inflow surges. In addition the mechanism of wave attenuation is described together with a summary of the development of the necessary unsteady flow equations. Details of the computer program TRANSCC are included together with the data preparation instructions. Limited experimental verification of the analysis is also presented based on transient flow depth measurements for hydraulic characteristics of surge flows which have been conducted as part of the test program for solid transport mechanisms in the Plumbing Research Laboratory of NBS CBT.

2. FLOW ATTENUATION IN LONG PARTIALLY FILLED PIPE FLOW

Gravity driven flow in partially filled pipes or open channels may be characterized by the observation that the flow depth may change in response to both the applied loading and the frictional forces acting on the fluid flow. In order to explain the mechanism of this depth change, or attenuation, observed in long channels or free surface pipe flow it is necessary to consider wave propagation in these flow regimes.

It may be shown [2] that in non rectangular channels the wave propagation velocity is related to flow depth via the channel geometry,

$$c = \sqrt{\frac{gA}{T}}$$

where T is the flow surface width and A is the flow cross section area, both functions of flow depth and channel geometry.

This implies that deeper waves travel faster than shallower waves and would thus overtake leading shallower water or conversely outdistance following shallower flow. Obviously this model is perceived in the flow by changes in the observed depth profile shape.

Figure 1 illustrates the propagation of both positive and negative waves in frictionless channels. If the wave front is considered to be made up of a large number of very small waves placed one on top of the other then it may be seen that, in the theoretically frictionless channel, the wave profile steepens for the positive wave and attenuates for the negative wave. The deeper waves in each case travel faster than the shallower waves, thus in the positive surge the crest overtakes the leading edge and the profile steepens. Alternatively for the negative surge the crest outdistances the trailing edge resulting in a spreading out of the wave.

The presence of frictional effects materially alters this situation. As the forces generated depend on the square of velocity the introduction of frictional effects results in modifications to both the positive and negative surge shape changes described above. Figure 1 illustrates the reduction in negative surge attenuation as the deeper wave, travelling at the higher velocity, is retarded relative to the shallower trailing waves and to its frictionless performance.

Similarly the steepening of the positive wave front is reduced and, depending on the channel friction, possibly attenuated as shown.

The effect of this mechanism on observed partially filled pipe flow is a progressively reducing depth downstream for a surge introduced into a long pipe, figure 2, associated with a reduction in the peak flow rate recorded at any downstream section.

This flow attenuation and reduced flow depth has direct implications on drainage system design, particularly in the context of water conservation.

Consider an isolated finite discharge introduced into a long drainage pipe. As this proceeds along the pipe, its depth decreases and the length of the water wave increases, i.e., the flowrate at any section is attenuated.

If the pipe is designed on the basis of a given number of such discharges with no allowance for either flow attenuation or the probability of simultaneous discharge then it will be seen that the pipe is either oversized or the maximum loading, allowing for a probability usage pattern for the appliances contributing to the loading, will be underestimated.

In the U.K. particularly this discussion has been represented by the numerical limit to the number of domestic dwellings that may be connected to a standard 100 mm drain. Current design recommendation could be substantially increased if flow attenuation and inflow probability were combined and included in the design calculations.

It has been shown [3] that the transport of solids through drainage systems is substantially dependent on flow depth so that the exclusion of depth attenuation calculations also indicates an enhanced probability of solid deposition in long pipes. These effects are naturally aggravated if water conservation proposals are accepted for existing installed systems, and reinforce the view that water conservation should also include a study of pipe sizing, leading either to possible reductions in standard pipe diameters or to increased appliance loading for existing pipework.

At present there is little experimental data on flow attenuation in long pipelines. Burberry [4] presented limited laboratory test results together with frequency of appliance operation tables that support the arguments above. However in this case laboratory tests are limited in their usefulness due to the complexity of the flow combinations possible in an installed system. For example the attenuation of an appliance discharge, such as a water closet (w.c.), can be measured in the laboratory in pipes at a range of gradients and lengths, however in practice this attenuated flow could be joined at some downstream location by another discharge emanating from another appliance. Thus if the benefits of flow attenuation are to be included in drainage design and conversely the maintenance problems inherent in disregarding this effect in a water conserving system are to be avoided, then it is necessary to develop a predictive technique that would include random flow additions in both time and location along the drainage system.

Due to the complexity of drainage systems in such building complexes as hospitals, this analysis would have to involve a computerized solution that would be based on the full unsteady flow equations. Such a solution would have to be capable of accepting multiple inputs to a branched system and would be expected to yield predictions of flow depths and velocities, including backflow at pipe junctions.

The current report presents a feasibility study based on the use of the method of characteristics to solve the unsteady flow equations and predict flow

attenuation for a pipe without branches. It is based on a preceding study of the use of this technique to determine the depth build up at a deposited stationary solid in response to a discharge moving along a drainage pipe [1].

3. DEVELOPMENT OF THE NUMERICAL SOLUTION

3.1 SUMMARY OF METHOD OF CHARACTERISTICS SOLUTION OF THE EQUATIONS DEFINING UNSTEADY FLOW IN PARTIALLY FILLED PIPE FLOW

Referring to figure 3, it has been shown [1] that the equations of motion and continuity may be expressed as

$$g \frac{\partial h}{\partial x} + g(S - S_o) + V \frac{\partial V}{\partial x} + \frac{\partial V}{\partial t} = 0 \quad (1)$$

$$VT \frac{\partial h}{\partial x} + T \frac{\partial h}{\partial t} + A \frac{\partial V}{\partial x} = 0 \quad (2)$$

These equations may be combined to form a total derivative expression

$$\frac{dV}{dt} + \frac{g}{c} \frac{dh}{dt} + g(S - S_o) = 0 \quad (3)$$

subject to

$$\frac{dx}{dt} = V \pm c \quad (4)$$

The wave speed being defined by

$$c = \sqrt{\frac{gA}{T}} \quad (5)$$

where V = local average flow velocity

c = local wave speed

h = local flow depth

S_o = pipe slope

S = slope of the local energy grade line = $\frac{n^2 V^2}{m^{4/3}}$, n the Manning coefficient and m the hydraulic mean depth

T = water surface width

A = water depth cross sectional area

Referring to figure 4, if the variables V and h are known at R and S then four equations may be written in terms of the unknowns at point P , by means of a first order approximation,

$$V_P - V_R + \frac{g}{c_R} (h_P - h_R) + g(S_R - S_o)\Delta t = 0 \quad (6)$$

$$x_P - x_R = (V_R + c_R)\Delta t \quad (7)$$

$$v_P - v_S - \frac{g}{c_S} (h_P - h_S) + g(S_S - S_0)\Delta t = 0 \quad (8)$$

$$x_P - x_S = (v_S - c_S)\Delta t \quad (9)$$

It is stressed that these equations are paired and that equations 6 and 8 only apply as long as equation 7 and 9 are satisfied. This introduces the characteristics lines C^+ and C^- , shown in figure 5.

It is also necessary that the time step Δt is sufficiently small for R and S (points in the $x-t$ plane) to fall within $\pm \Delta x$ of point P as shown in figure 4.

From figure 5 it will be seen, provided boundary equations governing the conditions at the extremities of the system are known, that an orderly solution may proceed yielding flow depth and velocity at each pipe section at each time increment.

The basis for the system boundary conditions are set out below.

3.2 PARTIALLY FILLED PIPE FLOW REGIMES

Two flow regimes may be identified for open channels or partially filled pipes:

(1) Subcritical flow, Froude $N^\circ = \frac{V}{\sqrt{gh}} < 1$

Here the local wave speed exceeds the flow average velocity, thus waves may be propagated both upstream and downstream in the flow, i.e., $c > V$.

(2) Supercritical flow, Froude $N^\circ > 1$

Here the local wave speed is less than the average flow velocity at that section and hence waves cannot be propagated upstream, i.e., $V > c$.

The flow regime applicable to any partially filled pipe flow may be determined by a comparison of the flow normal and critical depths as described, following the equations 10-15.

Under steady uniform flow conditions the force balance equation for an element of flow is normally expressed by the Chezy equation

$$V = C \sqrt{m S_0} \quad (10)$$

- m = hydraulic mean depth A/P , m
- S_0 = $\sin \theta$ - duct slope
- V = mean velocity m/s
- C = Chezy constant.
- P = pipe wetted perimeter.

The value of loss coefficient C was found by Manning to be dependent on hydraulic mean depth and duct surface roughness n . The Manning formula is the

simplest of the open channel equations:

$$v = \frac{1}{n} m^{2/3} S_o^{1/2}$$

$$Q = \frac{1}{n} A m^{2/3} S_o^{1/2} \quad (11)$$

where Q is the flow rate m^3/s
 A is the flow cross sectional area, m^2

The value of the Manning coefficient, n , varies with pipe or channel material. Chow [2] suggests values in the range 0.009 to 0.020 for materials commonly found in building drainage systems.

Equation 10 effectively determines the flow depth under steady, uniform conditions, only one value of h yielding the values of A and m necessary to satisfy the equation. As this depth is by definition constant downstream, $dh/dx = 0$, it must also be the terminal depth corresponding to the flow terminal velocity at that channel slope.

This depth, h_n , is commonly referred to as the normal depth.

The specific energy of the flow may be defined as

$$E = h + \frac{v^2}{2g} \quad (12)$$

where h = local flow depth, m
 v = local average flow velocity, m/s

It may be shown that for a rectangular channel, width w , that there are two possible depths for any particular value of E above a minimum.

$$E = h + \frac{v^2}{2g} = h + \frac{Q^2}{2gA^2}$$

with $A = hw$ for rectangular case, then

$$E = h + \frac{Q^2}{2g(hw)^2}$$

$$h^3 - Eh^2 + Q^2/2gw^2 = 0$$

For E constant, this equation has three roots, two real, one imaginary.

Figure 6 illustrates the alternate depths possible in such a situation and their significance in terms of the flow definition.

From equation 12 and figure 6 it may also be seen that the flow specific energy has a minimum value below which the given flow conditions cannot exist. In a general, non rectangular channel this value may be determined:

$$E = h + \frac{Q^2}{2gA^2}$$

$$\frac{dE}{dh} = 0 = 1 - \frac{Q^2}{gA^3} \frac{dA}{dh} \quad (13)$$

From figure 3

$$dA = T dh \quad (14)$$

where T is the surface width at any depth, h .

From equations (13) and (14) the minimum value of E will occur at a depth value, h_c , that satisfies the expression

$$1 - \frac{Q^2 T}{gA^3} = 0 \quad (15)$$

where T and A are both $f(h)$

This value of h is referred to as the flow critical depth h_c .

If the normal flow depth h_n exceeds h_c then the terminal flow would be termed subcritical, or tranquil flow. If h_n is less than h_c then the flow is termed rapid or supercritical.

It should be stressed that h_c is independent of pipe slope and pipe surface roughness; while the normal depth is dependent on both. Thus the same volume flow rate in any particular pipe may be rapid or tranquil depending on pipe slope, and similarly the same flow rate in a series of constant diameter pipes will be tranquil or rapid depending on roughness.

Pipes or channels in which rapid flow is normal are termed steep, pipes or channels in which tranquil flow is normal are termed of mild slope.

Figure 4 illustrates the importance of these two flow regimes on the solution of equations 6 to 9.

If $c > V$ then the conditions at P are determined by the intersection of the C^+ and C^- drawn from P into the AC and BC sections.

If $c < V$ then conditions in the downstream section BC cannot effect point P . The slope of the C^- characteristic, PS , becomes positive and both R and S lie in the AC section as shown.

Both subcritical and supercritical flow are encountered in the drainage applications considered and the equations derived below cover both conditions.

Referring to figure 4 for subcritical flow:

$$\frac{v_C - v_R}{v_C - v_A} = \frac{x_C - x_R}{x_C - x_A} = (v_R + c_R) \frac{\Delta t}{\Delta x}$$

$$\frac{c_C - c_R}{c_C - c_A} = \frac{x_C - x_R}{x_C - x_A} = (v_R + c_R) \frac{\Delta t}{\Delta x}$$

and $\frac{h_C - h_R}{h_C - h_A} = (v_R + c_R) \frac{\Delta t}{\Delta x}$

as $x_P = x_C$ and $x_P - x_R = (v_R + c_R)\Delta t$

Solution yields

$$v_R = \frac{v_c + \theta (-v_C c_A + c_C v_A)}{1 + \theta (v_C - v_A + c_C - c_A)} \quad (16)$$

$$c_R = \frac{c_c(1 - v_R \theta) + c_A v_R \theta}{1 + c_C \theta - c_A \theta} \quad (17)$$

$$h_R = h_C - (h_C - h_A)(\theta(v_R + c_R)) \quad (18)$$

where $\theta = \Delta t/\Delta x$

Similarly

$$v_S = \frac{v_c - \theta(v_c c_B - c_C v_B)}{1 - \theta(v_c - v_B - c_C + c_B)} \quad (19)$$

$$c_S = \frac{c_c + v_S \theta (c_C - c_B)}{1 + \theta (c_C - c_B)} \quad (20)$$

$$h_S = h_C + \theta(v_S - c_S)(h_C - h_B) \quad (21)$$

For the supercritical flow regime the equations determining R in figure 4 remain unchanged. The interpolation equations for S' in figure 4 may be determined by an identical technique to that shown above,

$$v_C - v_{S'} = (v_C - v_A) \theta (v_{S'} - c_{S'})$$

$$c_C - c_{S'} = (c_C - c_A) \theta (v_{S'} - c_{S'})$$

and $h_C - h_{S'} = (h_C - h_A) \theta (v_{S'} - c_{S'})$

Solution yields

$$v_{S'} = \frac{v_C(1 - c_A \theta) - v_A c_C \theta}{1 + \theta(v_C - v_A + c_A - c_C)} \quad (22)$$

$$c_{S'} = \frac{c_C + V_{S'} \theta (c_A - c_C)}{1 + c_A \theta - c_C \theta} \quad (23)$$

From equations 7 and 9 it will be seen that

$$\frac{dt}{dx} = \frac{1}{V + c} \quad (24)$$

hence if $(V + c)$ becomes large then Δt becomes small for a constant Δx . This implies that the progress of the numerical solution could become prohibitively slow for supercritical flow conditions. Fox [5] suggests a check within any program that will terminate the solution if Δt falls below a specified value, however this comment by Fox applies to the existing applications of the method of characteristics, which have been limited to large civil engineering open channel or river flooding flow problems. It is likely that the reduction in Δt will not be a significant problem with the relative values of V and c encountered in drainage sized pipe applications due to their dependence on pipe geometry and flow rate. This point will be returned to later in the discussion of the supercritical flow simulations.

The determination of conditions at P at time $t + \Delta t$ requires the following steps (i-iv), for either sub or supercritical flow conditions

- (i) All conditions known at time t for nodal points A, B, C etc, figure 4
- (ii) Values of V , h and c at interpolation points R, S, or S' calculated from equations 16 - 23.
- (iii) Using these values of V , h , and c the conditions at P, i.e. velocity V and depth h , at time $t + \Delta t$ are calculated by means of equations 6 and 8.
- (iv) The value of wave speed c at P at time $t + \Delta t$ is calculated from equation 5. The value of flow surface width and cross sectional area are calculated from flow depth, h , and the channel shape relationships, figure 7.
- (v) The sequence is repeated at each new time step.

3.3 APPLICATION OF THE METHOD OF CHARACTERISTICS SOLUTION TO DRAINAGE FLOW

For convenience the application of the solution developed above to drainage pipe flow may be considered under two headings, namely boundary conditions and characteristic equation solution at intermediate pipe sections. Both of these headings must be further subdivided depending on whether the flow is termed sub or supercritical.

The equations 6 to 9 may be restated as

$$\begin{aligned} V_P &= X_2 - X_1 h_P \\ x_P - x_R &= (V_R + c_R)\Delta t \end{aligned} \quad \left. \vphantom{\begin{aligned} V_P &= X_2 - X_1 h_P \\ x_P - x_R &= (V_R + c_R)\Delta t \end{aligned}} \right\} \text{for } C^+ \quad (25)$$

$$\begin{aligned} V_P &= X_4 + X_3 h_P \\ x_P - x_S &= (V_S - c_S)\Delta t \end{aligned} \quad \left. \vphantom{\begin{aligned} V_P &= X_4 + X_3 h_P \\ x_P - x_S &= (V_S - c_S)\Delta t \end{aligned}} \right\} \text{for } C^- \quad (26)$$

where $X_1 = g/c_R$

$X_3 = g/c_S$

$X_2 = V_R + g \frac{h_R}{c_R} - g(S_R - S_0)\Delta t$

$X_4 = V_S - g \frac{h_S}{c_S} - g(S_S - S_0)\Delta t$

It will be noted that these equations apply in either subcritical or supercritical flow, the interpolated values of the conditions at S or S' being sufficient to define the flow regime, figure 4.

3.3.1 Initial Steady Conditions Along the Pipe Length

As will be seen from figure 5 the initial conditions along the whole pipe length at time $t = 0$ must be known in order for the solution to proceed. It is therefore necessary to calculate the steady state flow velocity and depth throughout the pipe length initially, together with the initial wave speed. This process may be carried out by the following steps.

- (i) Determine the steady flow normal and critical depths as set out previously. This determines whether the flow is subcritical or supercritical.
- (ii) For supercritical flow the normal flow depth may be assumed to apply throughout the pipe length. As the velocity exceeds the wave speed there is no effect propagated upstream from the pipe discharge point. This implies that the flow leaves the pipe at normal depth and for a known flow rate and pipe dimension allows the local velocity and wave speed to be calculated along the whole pipe length.
- (iii) For subcritical flow the initial water surface profile is more complicated as the effect of the pipe discharge is propagated upstream. In subcritical flow it has been found that the depth of flow is at its critical value at the discharge point with the water depth then rising upstream until the normal steady flow depth is achieved. Calculation of this depth profile is presented in [6] and summarized below in terms of the gradually varied flow profile prediction technique.

Gradually varied flow is steady non-uniform flow of a special type. The flow parameters are assumed to change slowly, if at all, in the flow direction. The basic assumption in the treatment of this type of flow is that the local head loss at any section is given by the Manning expression (11), for the identical local flow depth and rate under assumed steady, uniform flow conditions.

Depth profile predictions by numerical integration are based on this assumption, expressed in terms of figure 8 by

$$\frac{d}{dL} \left\{ \frac{V^2}{2g} + (Z_0 - S_0L) + h \right\} = - \left\{ \frac{nQ}{Am^{2/3}} \right\}^2 \quad (27)$$

where $(Z_0 - S_0L)$ is the elevation at distance L along the channel, measured in the downstream direction; S_0 is $\sin \theta$, channel bed slope,

$$\text{hence } - \frac{V}{g} \frac{dV}{dL} + S_0 - \frac{dh}{dL} = \left(\frac{nQ}{Am^{2/3}} \right)^2 \quad (28)$$

and as, $Q = VA$

$$\frac{dV}{dL} A + V \frac{dA}{dL} = 0$$

and as $\frac{dA}{dh} = T$ from equation 5 it follows that

$$\frac{dV}{dL} = - \frac{V}{A} \frac{dA}{dL} = - \frac{VT}{A} \frac{dh}{dL} = - \frac{QT}{A^2} \frac{dh}{dL}$$

and substituting in equation 28 yields

$$\frac{Q^2 T}{gA^3} \frac{dh}{dL} + S_0 - \frac{dh}{dL} = \left\{ \frac{nQ}{Am^{2/3}} \right\}^2 \quad (29)$$

$$dL = \left\{ \frac{1 - Q^2 T / g A^3}{S_0 - (nQ / Am^{2/3})^2} \right\} dh$$

$$L = \int_{h_0}^{h_1} \frac{1 - Q^2 T / g A^3}{S_0 - (nQ / Am^{2/3})^2} dh \quad (30)$$

where L is the distance between two known depths h_0, h_1 .

Figure 9 illustrates this numerical integration, which may be conveniently achieved by Simpson's rule.

The numerator and denominator of equation 30 will be recognized as the equations determining the critical and normal flow depths in an open channel.

When the term $(1 - Q^2T/gA^3)$ is zero the flow is at critical depth, i.e., there is no change in L for a change in h.

When the term $S_o - (nQ/Am^{2/3})^2$ is zero uniform flow depth is achieved, i.e., there is no change in h for a change in L.

The initial depth at each section Δx apart along the pipe may then be calculated from the profile produced by the integration of equation 30. Flow velocity is then calculated based on a constant flow rate through the pipe and similarly wave speed is determined based on flow depth and channel geometry.

Once the initial flow depth, velocity and wave speed have been determined the unsteady flow calculation procedure may begin.

3.3.2 Internal or Nodal Points

Simultaneous solution of equations 25 and 26 at all points Δx apart between $x = \Delta x$ and $x = (L - \Delta x)$ will yield the required values of flow depth and velocity at the end of each time step. Wave speed may then also be determined from equation 5. This process applies to either sub or supercritical flow conditions as the particular regime is represented in the interpolations required to fix points R, S or S', figure 4.

3.3.3 Entry Boundary Condition, Supercritical Flow

In this case the inflow profile alone determines the flow depth at pipe entry as downstream conditions, that would have been represented by the C^- characteristic in subcritical flow, cannot effect the flow conditions at the upstream boundary, as by definition the flow velocity exceeds the wave speed.

Hence the boundary condition is obtained from the flow profile $Q = f(t)$

solved with the normal depth expression

$$Q = \frac{1}{n} A m^{2/3} S_o^{1/2}$$

where A and m are both $f(h)$. This equation may be rewritten in the form

$$1 - \frac{(nQ)^2}{A^2 m^{4/3} S_o} = 0 \quad (31)$$

and this boundary expression may be solved at each time step with a known Q by the bisection technique; this technique is described later.

3.3.4 Entry Boundary Condition, Subcritical Flow

For subcritical flow the downstream conditions do contribute to the entry flow depth and velocity. In this case the inflow profile $Q = f(t)$ is solved with the C^- characteristic

$$Q = f(t) = V_1 A_1$$

$$V_1 = X_4 + X_3 h_1$$

$$Q(t) = A_1 (X_4 + X_3 h_1) \quad (32)$$

where suffix 1 refers to the entry boundary location and $A = f(h)$ dependent on the pipe cross sectional geometry.

In the form

$$Q(t) - f(h_1)(X_4 + X_3 h_1) = 0 \quad (33)$$

this boundary equation may be solved by the bisection technique.

3.3.5 Exit Boundary Condition, Supercritical Flow

As the flow velocity exceeds the local wave speed the exit boundary condition may be determined in the same manner as the upstream nodal points, namely by the simultaneous solution of the C^+ and C^- characteristics. With reference to figure 4 both the R and S' points lie upstream of the pipe exit.

The exit condition may be included in the nodal point calculations for the supercritical flow case, no separate exit subroutine being necessary in the program as equations 25 and 26 are sufficient.

3.3.6 Exit Boundary Condition, Subcritical Flow

At pipe exit in the subcritical flow regime the flow depth approaches the critical depth value, given by zero value of equation 15:

$$\frac{Q^2}{g A_{crit}^3} T_{crit} = 1,$$

where A and T are $f(h)$

This condition may be solved with the C^+ characteristic

$$V_{N+1} = X_2 - X_1 h_{N+1}$$

where $N = N^\circ$ of pipe length sections, Δx .

The boundary condition becomes

$$[(X_2 - X_1 h_{N+1}) A_{N+1}]^2 \frac{T_{N+1}}{g A_{N+1}^3} - 1 = 0 \quad (34)$$

Solution may again be achieved by use of the bisection method together with the use of the area to depth relationship for the channel.

4. CALCULATION TECHNIQUES AND PRESENTATION OF RESULTS

4.1 DETERMINATION OF NORMAL AND CRITICAL DEPTHS

The bisection method was used to solve the equation defining both critical flow depth

$$X = 1 - Q^2 T / g A^3$$

and normal flow depth

$$Y = S_o - (n Q / A m^{2/3})^2.$$

that feature as boundary conditions.

It may be assumed that both X and Y have zero values for some value of depth h in the range $0 < h < D$ for the pipe case.

This initial interval is bisected and $h = D/2$ used to evaluate X, Y. If the resulting values are positive then the root is less than the midpoint and the upper limit is reset equal to the h value just used and the remaining interval 0 to D/2 bisected. The process repeats until a root is obtained. If the X or Y value had been negative then the root would be greater than the trial h value, in this case the lower limit is reset to the trial h value and the interval bisected.

Due to the need to include the area depth relationship this solution must be undertaken by an iterative process. The time taken depends on the complexity of the area-depth function.

4.2 NUMERICAL INTEGRATION FOR SURFACE PROFILES

The integration of the position vs depth profile

$$L = \int_{h_1}^{h_2} \frac{1 - Q T^2 / g A^3}{S_o - (n Q A m^{2/3})^2} dh$$

is achieved by means of Simpson's Rule. Let the integral $X = \int_{h_0}^{h_1} F(h) dh,$

than if the interval $h_1 - h_0$ is divided into 2 equal increments, the value of X is given by

$$X = \frac{1}{3} dh [F(h_0) + 4F(h_0 + dh) + F(h_0 + 2 dh)]$$

As the integration progresses the length traversed may be accumulated as $L_{n+1} = L_n + X$ at the completion of each integration.

4.3 CHOICE OF TIME STEP

Referring to figure 4 it will be seen that the time step chosen must be such that the points R and S fall within $\pm \Delta x$ of point P. In order for this to occur for all sections along the pipe it follows that

$$\Delta t = \frac{\Delta x}{(V + c)_{\max}} \quad (35)$$

This expression yields the smallest possible time step as the maximum values of flow velocity and wave speed at any pipe section has been used.

In order to ensure that the computation proceeds as quickly as possible the computer program presented calculates a new time step magnitude at each time increment so that the time step increases when V and c decrease but decreases to maintain a stable solution when V and c are increasing in response to an inflow surge.

4.4 PRESENTATION OF RESULTS

The objective of the simulated pipe flow data developed from use of the Fortran computer program TRANSCC, run on the NBS CBT Perkin Elmer 732 computer, was to identify the potential of the method of characteristics solution for flow attenuation prediction and also to highlight any limitations inherent to the technique.

The following test cases were investigated and are reported here:

- (1) Investigation of effect of the number of nodes, i.e., pipe computational section length Δx , for subcritical flow, pipe slope 1/300, diameter 0.1 m, length 5m, and for supercritical flow, pipe slope 1/40, diameter 0.1 m, length 5 m.
- (2) Investigation of effect of peak flow duration, either 2 or 6 seconds at 1.0 l/s at pipe slopes of 1/100 or 1/300, pipe diameter 0.1 m, pipe length 5 m.
- (3) Effect of pipe gradient on flow attenuation in a 30 m long, 0.1 m diameter pipe, pipe slopes of 1/40, 1/100, 1/300.
- (4) Effect of pipe diameter on flow attenuation, pipe diameters 0.15 m, 0.1 m, 0.075 m at 1/40, 1/100, 1/300 slopes, 30 m long pipe.
- (5) All simulations above employed a constant Manning coefficient of 0.015. The effect of varying Manning coefficient from 0.009 to 0.020 in a 0.1 m diameter, 15 m long pipe at 1/100 slope was also investigated.
- (6) The effect of the initial flow rate assumed in the pipe was studied, varied from 0.2 l/s to 0.05 l/s in a 0.1 m diameter pipe, 15 m long, at 1/300 and 1/40 pipe gradient subjected to peak inflow rates of 1.2 and 4.2 l/s.

The results of these simulations are presented in graphical form and are discussed.

5. DISCUSSION OF UNSTEADY FLOW SIMULATION RESULTS

5.1 INFLUENCE OF SPECIFIED TIME INTERVAL GRID SIZE ON PREDICTED FLOW PARAMETERS

In order to apply the solution technique described the pipe length must be split into a number of equal increment at length Δx . The calculation time is dependent on this subdivision length and on the local wave speed and flow velocity via the expression

$$\Delta t = \frac{\Delta x}{V + c}$$

Hence for a given pipe length and duration of flow simulation the computing time and consequently cost, is determined by the choice of the number of pipe sections adequate to provide an acceptable prediction of the flow parameter variation with time.

Figure 10 illustrates the effect of dividing a 5 m length of pipe, into 5, 10 or 30 equal computational subdivisions, Δx varying from 1 m to 0.167 m.

The variations in predicted flow rate at each node along the pipe length may be explained entirely in terms of the interpolation required to yield the base conditions for each computing time step, outlined in figure 4.

The interpolation in figure 4, necessary to determine conditions at R and S at time t, from calculated values of depth, velocity and wave speed at A, B and C, effectively assumes that disturbances arriving at A, B or C at time t effect conditions ahead of their true positions, namely at R and S.

Therefore the initial depth increase propagated in the pipe flow by the rise in the inflow curve, $Q = f(t)$, would be expected to register earlier at any particular section if the number of pipe sections were small. With larger pipe section lengths the apparent disturbance propagation speed is increased due to this interpolation technique.

Similarly any decrease in depth at the inlet would also be recorded earlier at a downstream section if the Δx chosen were large. As the depth and flow velocity predictions may be thought of as summations of positive and negative change waves moving back and forth along the flow it is therefore to be expected that the peak values predicted for flow depth and velocity will increase towards a true limit as the pipe computing section length decreases.

These effects are clearly seen in the simulated results presented in figure 10. As the number of pipe sections increases from 5 to 30, so does the peak flow rate predicted, although the change between 5 and 10 sections is several times the change between 10 and 30 sections, indicating an approach to a true prediction limit.

Figure 11 repeats this assessment for a supercritical flow in a pipe at a 1/40 gradient. Here there is little attenuation in the first 4 m length when

compared to the very pronounced attenuation in the 1/300 gradient pipe of figure 10. This lack of attenuation is explainable in terms of the frictional and mass forces acting. The effects of Δx choice however remain as described for the 1/300 pipe case, earlier depth changes being detected with the larger pipe sections together with reduced peak flow rate predictions.

Figures 12 and 13 illustrate the depth changes along both the 1/40 and 1/300 pipe lengths for the inflow surge considered above. One point mentioned in the derivation of the flow boundary conditions is clearly demonstrated by these results, namely the initial water surface profile and the associated exit depth criteria.

For the 1/300 gradient pipe the flow is subcritical and hence the depth decreases at exit to the appropriate critical value. Figure 12 illustrates this profile for the steady initial flow of 0.1 l/s calculated by the gradually varied flow analysis described. The flow in the 1/40 pipe, figure 13 is by contrast supercritical and hence the flow depth along the whole pipe length remains at its normal value at all pipe sections, this depth being by definition both less than the critical depth appropriate to this pipe slope, diameter and flow rate and less than the corresponding normal depth in the shallower gradient, 1/300, pipe.

The choice of incremental length and the associated time step is to some extent a matter of experience. In general the flow simulations presented in this report were carried out with an incremental length of 0.5 m, this length being felt to be a reasonable compromise between short computer running time and an adequate representation of the flow depth and velocity time profiles.

5.2 INFLUENCE OF SURGE DURATION ON PARTIALLY FILLED PIPE FLOW RESPONSE

In a study of surge wave propagation Wyly [7] noted that the peak surge depth was dependent on the duration of the surge flow. This effect is clearly demonstrated in figures 14, 15, and 16, by means of a comparison of the attenuation in peak flow rates predicted at pipe slopes of 1/100 and 1/300 for two surge durations.

It will be seen that the effect of extending the duration of the inflow peak rate of 1 l/s from 2 to 6 s is to increase substantially the peak flow rate predicted at the downstream pipe sections. Examples have been taken at 2 and 4 m from the pipe entry.

This effect is to be expected and is in fact due to the flow establishment response characteristic of the pipe system. Obviously if the peak inflow of 1 l/s was held constant for a sufficient period then the flow in the pipe would become steady at this new flow rate, the water surface profile in the subcritical regime assuming the new 1 l/s characteristic normal depth with a progressive reduction to critical depth at the pipe exit.

5.3 INFLUENCE OF PIPE SLOPE, DIAMETER AND ROUGHNESS ON THE PREDICTED VARIATIONS IN FLOW DEPTH AND VELOCITY

The attenuation in flow depth and flow rate predicted by the unsteady flow analysis are caused by the balance of frictional and mass forces acting on the fluid. Within the model these friction forces are represented by the appropriate steady flow loss calculated from Mannings equation 11, but utilizing the flow velocity and depth at the particular pipe location and time step under consideration. Thus the variations in attenuation would be expected to follow the dependencies inherent in Mannings expression, namely friction forces dependent on pipe slope, roughness and diameter.

Figure 17 illustrates the attenuation in peak flow rate at four locations at 6 m intervals along a 30 m pipe at a range of gradients, 1/40, 1/100, 1/300. For this simulation pipe roughness and diameter were held constant. Two effects are clearly visible as gradient is reduced, namely the reduction in peak flow rate and the progressively later occurrence of this peak flow, indicating the dependence of flow velocity on pipe gradient.

Figures 18 and 19 illustrate the propagation of the surge wave at the three pipe gradients. Initially the water surface profiles at the three gradients are at normal depth with a reduction to critical depth at pipe exit in the subcritical flow cases, 1/100 and 1/300. As the wave travels along the pipes it will be noted that the wave progresses most rapidly in the steeper pipe, again this effect reinforces the forward movement of the peak flow rate noted in figure 17 and is predictable from the Manning expression dependency.

Figure 20 presents the peak flow rate for the 0.1 m diameter pipe from figure 17 in comparison with the predicted peak flows in 0.15 m and 0.075 m diameter pipes. At each of the three gradients considered the attenuation effect is least in the 0.15 m pipe and greatest in the 0.075 m pipe. Again this effect would be expected from the frictional forces acting for constant pipe slope and roughness.

Based on these observations it would be expected that attenuation would also be dependent on roughness, as represented by the Manning coefficient. Generally, in the simulations reported a constant value of Manning coefficient of 0.015 has been employed. This value is appropriate to cast iron pipe, Chow [2], and as such would be representative of many drainage applications. Figure 21 illustrates the effect of reducing pipe roughness to a Manning coefficient of 0.009 representative of very smooth bore glass or plastic drainage piping, and increasing to value of 0.02 representing aged piping. A pipe gradient of 1/100 was chosen to illustrate both the dependence of flow normal depth on pipe roughness and slope and the fact that subcritical or supercritical flow may be established in a constant slope pipe dependent only on pipe roughness. It will be noted from figure 21 that subcritical flow is established at Manning coefficients of 0.015 and above, supercritical flow at Manning coefficients of 0.012 and below.

Figure 21 also indicates the depth of flow dependence on pipe roughness, the smoother pipe featuring the shallower flow. Again this could be predicted for

a given flow rate in a pipe of constant gradient from the Manning equation for steady uniform flow.

5.4 INFLUENCE OF INITIAL AND RESIDUAL STEADY FLOW ON THE PEAK FLOW AND DEPTH PREDICTIONS

It has been shown that in order to utilize the method of characteristics solution of the unsteady flow equations it is necessary to establish the flow depth and velocity at all points along the pipe at time zero. In the simulations presented in this report the initial conditions have been chosen to represent a steady low flow rate through the system. Initial conditions are of course not limited to such a steady flow; however, this is by far the simplest base condition to employ.

It might appear therefore that the need to assume an initial flow in the system is a major limitation to the application of this analytical technique, however this may be shown not to be the case. The objective of the technique development reported was to provide a means of including the beneficial effects of flow attenuation on the design of long drainage pipes within, or collecting flow from, complex building drainage networks. A cursory study of the usage patterns of appliances within any complex building, such as a hospital, or domestic network serving a large number of living units, will indicate that such a system would be consistently carrying water at some minimum flow rate so that the response of the system to a surge input could be reasonably modelled by means of the techniques described.

Thus the initial constant flow rate in the region bounded by 0.05 to 0.2 l/s is reasonable as test conditions for the numerical solutions.

Similarly most appliance flow discharge profiles feature long, low flow, "tails", this is especially the case for such appliances as bathtubs and basins, thus the solution may be allowed to run for a given time period at a final value of steady flow and still be representative of actual flow conditions.

These constraints apply rather more to the test simulations included in this report than to the use of the techniques in a full system analysis as in the latter case the usage pattern of the system appliances would provide a continuous unsteady flow input to the system.

Figure 22 illustrates the peak flow rate and depth response predicted along a 20 m long, 0.1 m diameter pipe set at gradients of 1/40 and 1/300, during and following an input surge of 4.2 l/s. The initial and final steady flow values, assumed in the simulation, were set at 0.05, 0.1 and 0.2 l/s for each pipe slope. It may be seen that the maximum flow rate and depth achieved in the system at, or close to, pipe entry remains unaffected by these steady flow initial and final conditions. There is a variation in peak flow rate and depth achieved along the length of the pipe however, and this is entirely predictable in terms of the final steady state value being imposed on the system. Obviously the lower final flow rate of 0.05 l/s imposes a more rapid attenuation on the system when compared to the higher values of 0.1 and 0.2 l/s.

Theoretically there is no lower limit to the chosen value of final steady flow, however it should be noted that the peak flow rate to be expected in a building drain of these diameters would be in the range 8 to 10 ℓ/s , so that 0.05 ℓ/s represents a very small percentage.

Although the necessity to provide an initial and final flow rate along the system is a limitation on the technique, it is unlikely that this will be in anyway detrimental to the application of the developed technique to actual system analysis.

5.5 ESTIMATE OF COMPUTER RUN TIME

The program TRANSCC is included in an appendix to this report. The run time of the program is dependent on the number of pipe sections chosen to represent the pipe being studied. During the duration of this study the program was run on the NBS CBT Perkin Elmer 732 computer. It was found that a 30 m pipe made up of 60 pipe sections could be studied for a real time of 200 seconds for a computer run time of 15 minutes if no interruptions due to other users programs were experienced. It is clear therefore that the shorter length and real time duration cases were run in 2 to 3 minutes of computer time. In view of the fact that the machine used was by no means the fastest available it is considered that the technique developed is practical in terms of usability costs as a design tool.

6. EXPERIMENTAL VERIFICATION

The simulated flow attenuation results presented and discussed in the proceeding section have indicated that the technique developed is capable of providing flow rate, depth and velocity predictions as a surge wave moves along a drainage pipe at a range of slopes, roughness coefficients and diameters.

Experimental verification of the accuracy of these predictions for both subcritical and supercritical flow regimes will be a further stage in this work, however limited verification was possible utilizing an existing NBS CBT test rig designed to study solid transportation under controlled solid geometry conditions. Figure 23 summarizes the test rig and associated instrumentation. The discharge profile from the supply tank into the test pipe was obtained from the tank depth vs time curve as shown. This profile was then used as input to the simulation program TRANSCC. The depth vs time recordings at four stations along the test pipe were produced by means of an array of water sensing pins set at opposite pipe wall locations providing alternately 0.5 cm intervals around the pipe circumference at four locations as shown in figure 23. A d.c. current summing amplifier was employed to provide a depth sensitive signal, as illustrated in figure 23 and presented in figure 24 in comparison with predicted depth profiles at 4 adjacent points along the pipe. The program as used employed 30 pipe sections to simulate the 5.5 m length, however predicted results were only output at one tenth pipe length locations, although the program output could in the future be adapted to point predictions at a series of predetermined locations as an alternative.

The comparison between observed and predicted depths is in general encouraging; however, a number of points require clarification. The pipe slope was measured at 0.02, the Manning coefficient was assumed to be 0.012 based on available data; however, the results tend to indicate that the Manning coefficient was overestimated. The comparison indicates a progressive lag between observed and predicted depth, most noticeable at the 4.9 m station. A reduction in Manning coefficient would also tend to reduce peak depth predictions, however it is likely that the pins tend to yield overestimates of flow depth due to meniscus effects.

Similarly errors in the inflow profile, represented in figure 23, may be seen to contribute to the depth variations close to pipe entry, particularly in the supercritical flow regime where depth is entirely dependent on the upstream flow, represented in figure 24.

The depth comparison at the first pin station, at 0.64 m, indicates a rather more rapid rise in depth than that predicted. It is likely that the local flow close to pipe entry is subject to splashing and local waves not capable of simulation in the current program. As expected these local effects subside before the second pin station at 0.95 m is reached.

The inflow profile employed to derive the predictions is shown in figure 23, however in order to meet the simulation requirements the flow is assumed to continue at 0.01 l/s beyond the completion of the supply tank discharge at 7 seconds, as shown in figure 24. To some extent this requirement contributes

to the depth lag between observed and predicted traces, particularly at the final pin station. A final steady flow of 0.01 l/s in a 0.1 m diameter pipe is equivalent to a depth of 0.0027 m and accounts for a major portion of the divergence between observed and predicted depths at this station beyond the 20 second time point. As discussed previously this effect is a more serious defect in the evaluation of the artificial single surge case in the laboratory than it would be in practice in the study of a complex pipe network due to the usage patterns of appliances discharging to the system.

In general the results of the limited experimental verification suggest that the simulation and predictive techniques developed are capable of yielding information as to flow depth attenuation. A more detailed experimental program employing longer pipes, gradient adjustment, flow velocity and depth measurements and possible variation of pipe diameters and materials will be considered as an extension to the initial study reported.

7. CONCLUSION AND FURTHER WORK

The simulation of flow attenuation presented in this study has shown that the method of characteristic solution technique applied to the equations defining unsteady flow in partially filled pipe flow is capable of providing data on flow attenuation in long drainage pipes. A program of simulated flow tests indicated the generally expected relationships between flow attenuation and pipe diameter, gradient and roughness. Solutions to both subcritical and supercritical flow regimes were developed and tested in flow simulations.

Limited experimental verification was also undertaken and, within the limits imposed by pipe length and inflow profile measurement, the predicted depths were found to agree well with the measured time dependent variations.

As a result of the study reported further development of the technique is suggested to include multiple flow input to a branched pipe system. Similarly, an extended experimental program is proposed to further verify the accuracy of the flow attenuation predictions made practical by the reported techniques.

8. REFERENCES

- [1] Swaffield, J. A., "An initial study of the application of the numerical method of characteristics to unsteady flow analysis in partially filled gravity drainage sized pipes," NBS Report, August 1980.
- [2] Chow, V. T., "Open channel hydraulics," McGraw Hill, 1970.
- [3] Swaffield, J. A. and Marriott, B. S. T., "An investigation of the effect of reduced volume w.c. flush on the transport of solids in above ground drainage systems." CIB W62 meeting, Brussels, 1979.
- [4] Burberry, P., "Techniques for the estimation of flows in foul drains in the light of present water conservation proposals." CIB W62 meeting, 1979.
- [5] Fox, J. A., "Hydraulic analysis of unsteady flow in pipe networks." Macmillan Press, London, 1977.
- [6] Swaffield J. A., "Prediction of the hydraulic jump location following a change of slope in a partially filled drainage pipe," NBS Report, August, 1980.
- [7] Wyly, R. S., "Investigation of the hydraulics of horizontal drains in plumbing systems," NBS Monograph 86, 1964.

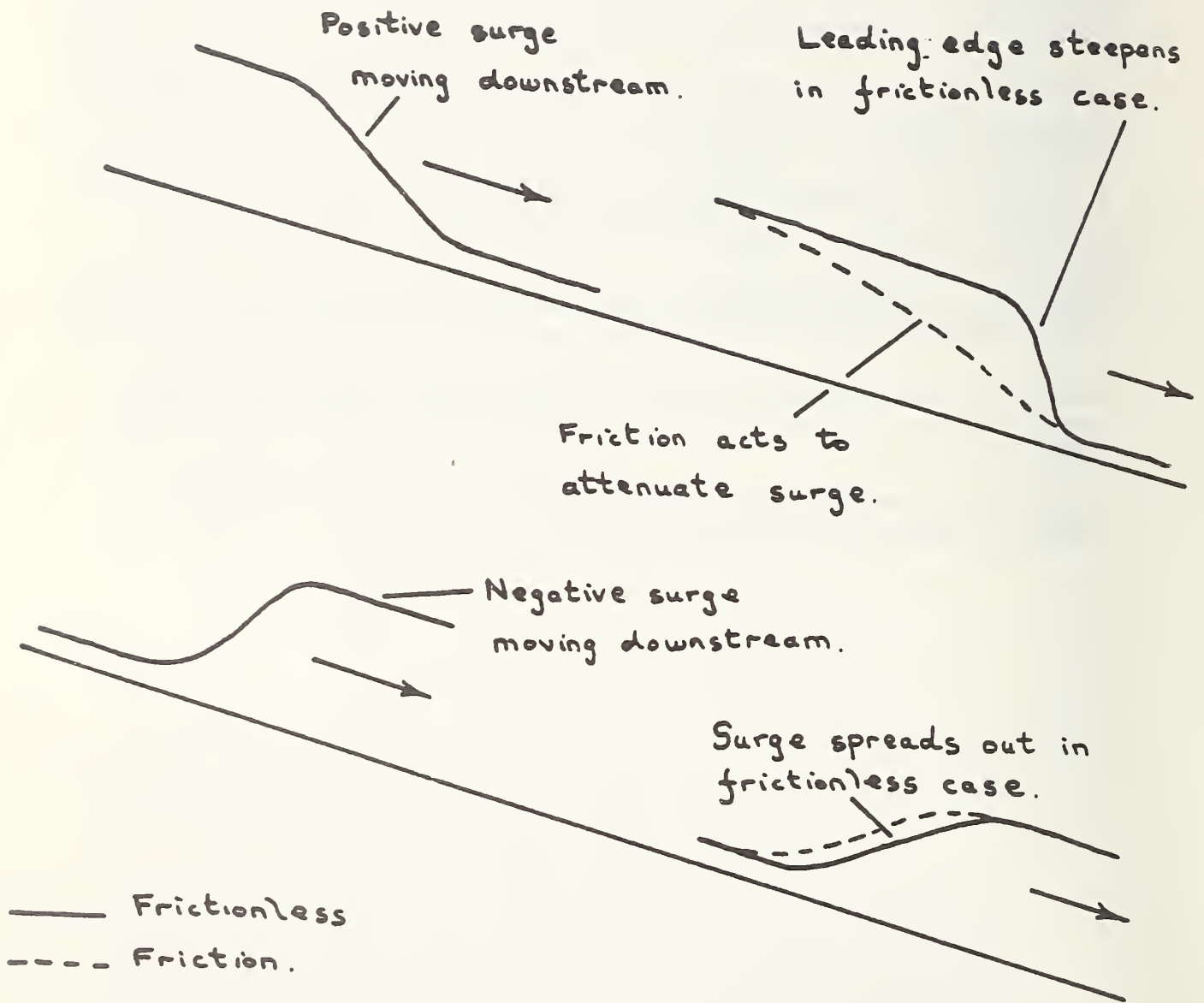


Figure 1. Propagation of positive and negative surges in partially filled pipe flow

Depth $h_1 > h_2$
 Flow duration $T_1 < T_2$
 local flowrate $Q_1 > Q_2$

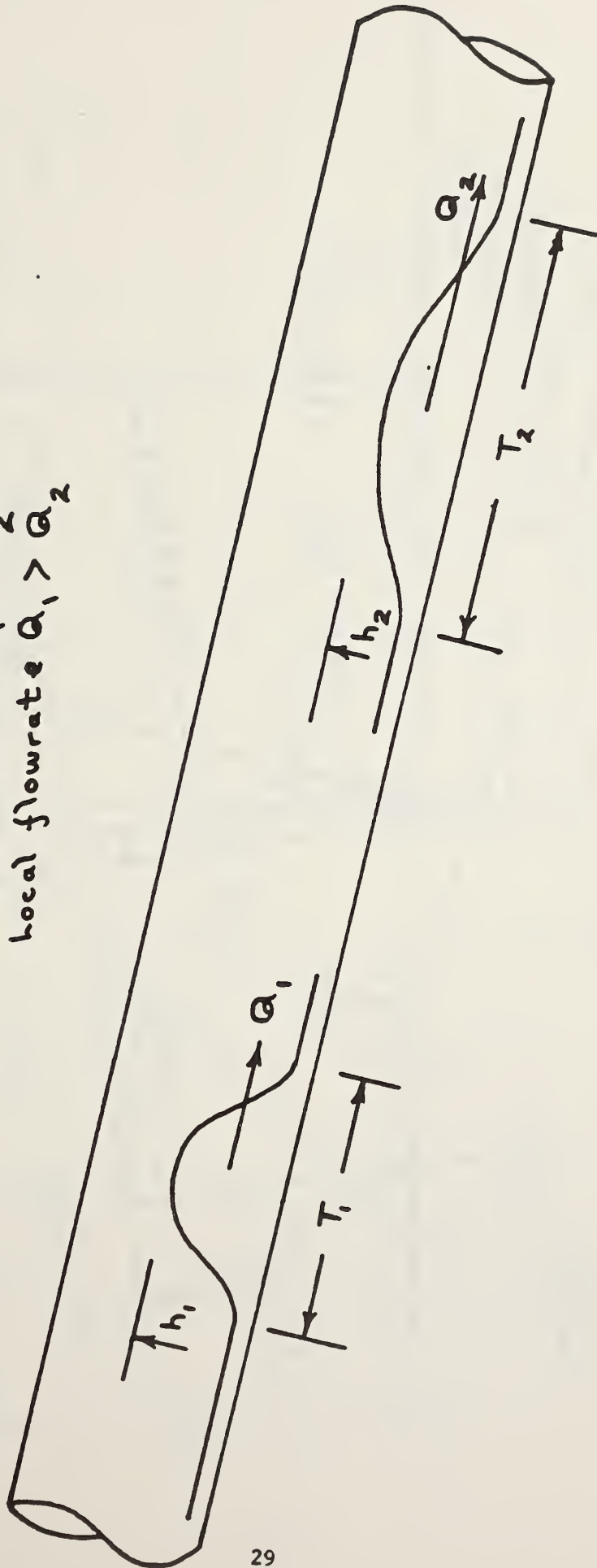
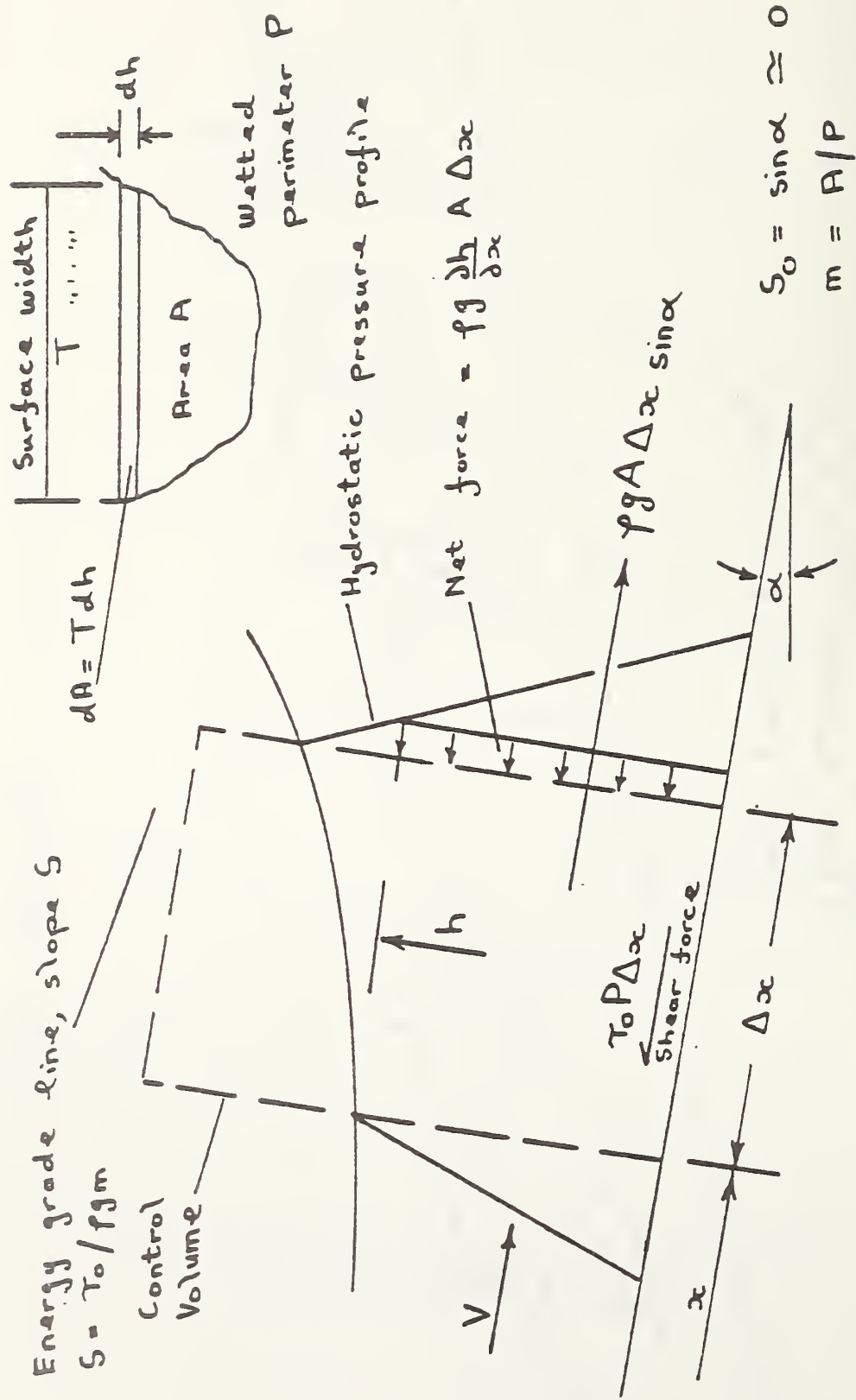
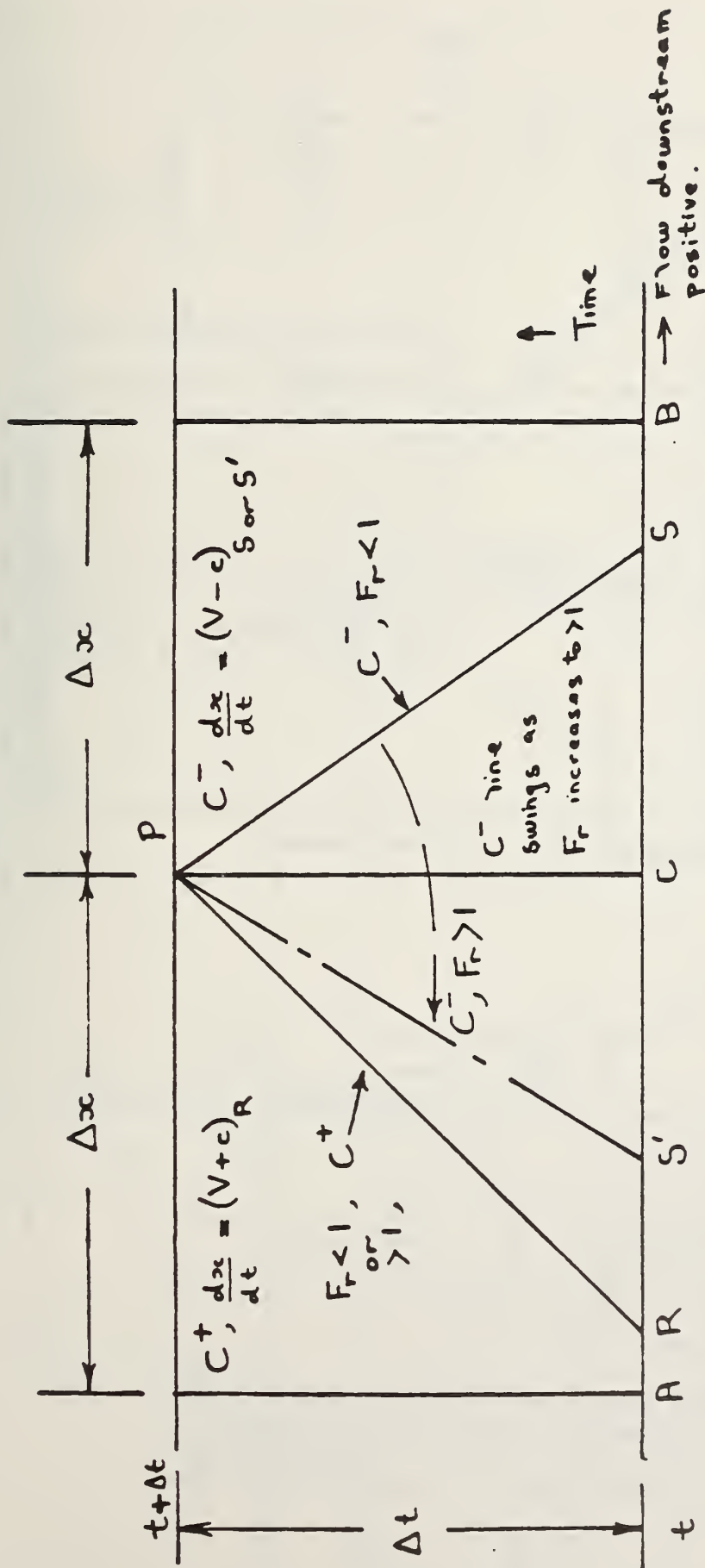


Figure 2. Surge attenuation as observed in drainage pipe flow



Note 2nd order terms neglected

Figure 3. Application of momentum equation to unsteady flow in a general open channel



$F_r = \text{Froude No.}$ < 1 subcritical flow, S lies in downstream section CB
 > 1 supercritical flow, S' lies in upstream section AC.

Figure 4. Modification to specified time interval grid for sub and supercritical flow regimes

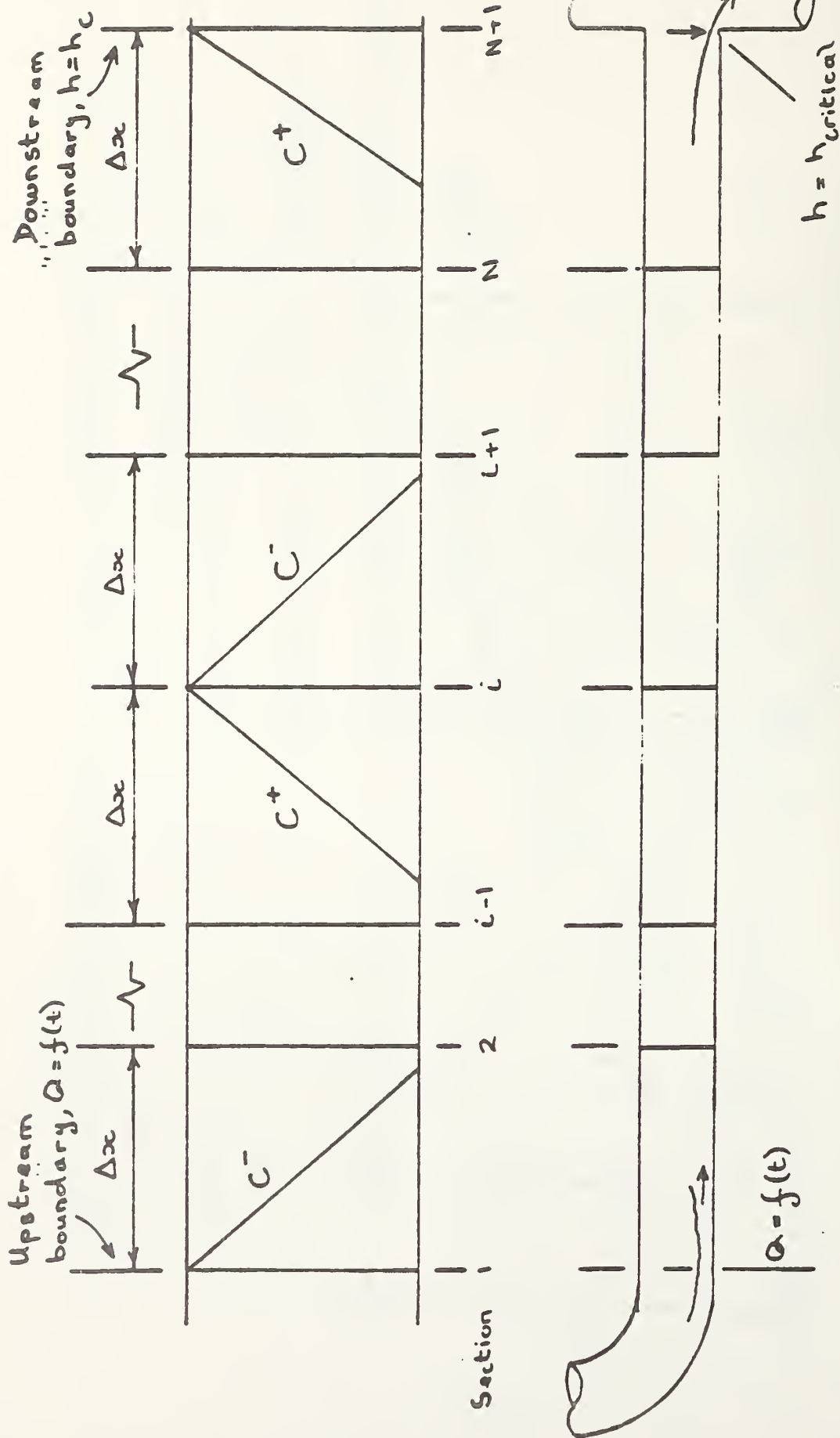


Figure 5. Application of specified time interval grid to subcritical partially filled pipe flow with known entry and exit boundary equations

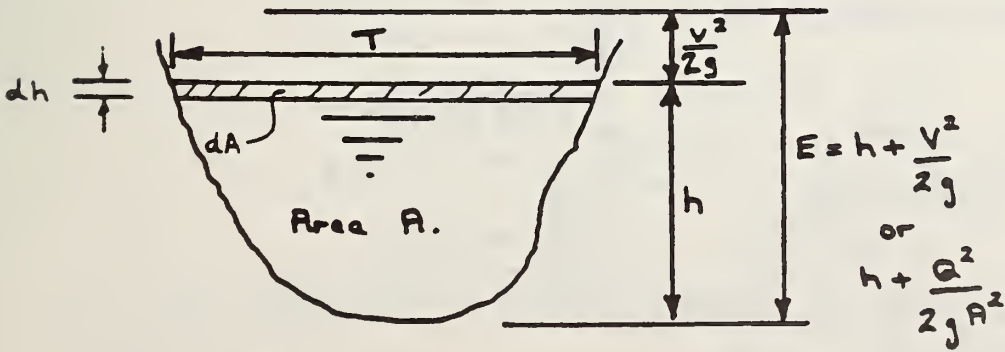
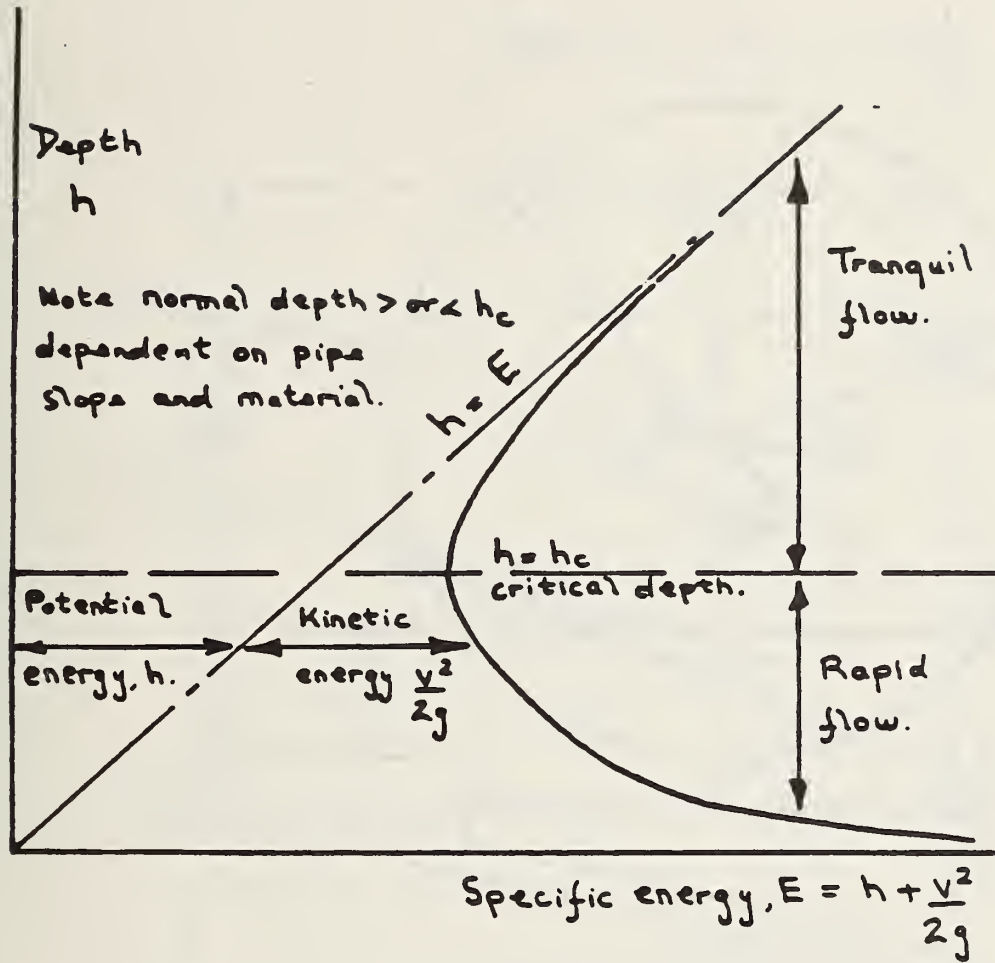
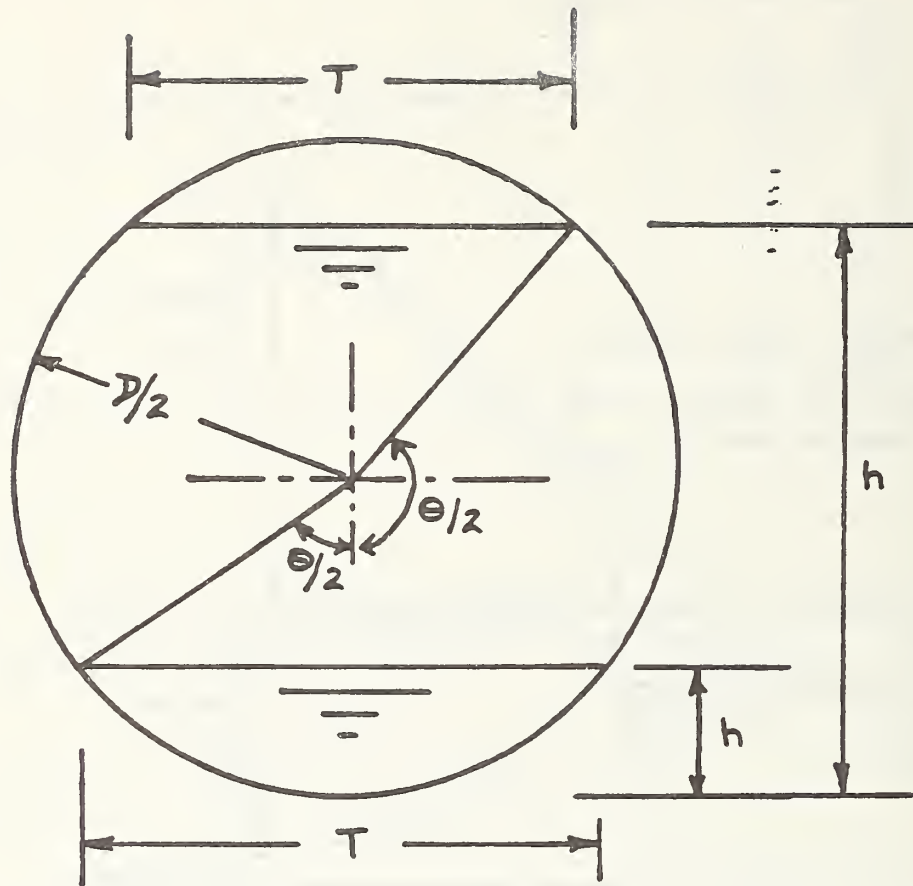


Figure 6. Relationship between flow specific energy and flow depth, illustrating the boundary between sub and supercritical flow regimes



Depth = h
 Subtended angle = θ
 Flow cross section area = $\frac{D^2}{8} (\theta - \sin \theta)$

Surface width = $2\sqrt{h(D-h)}$

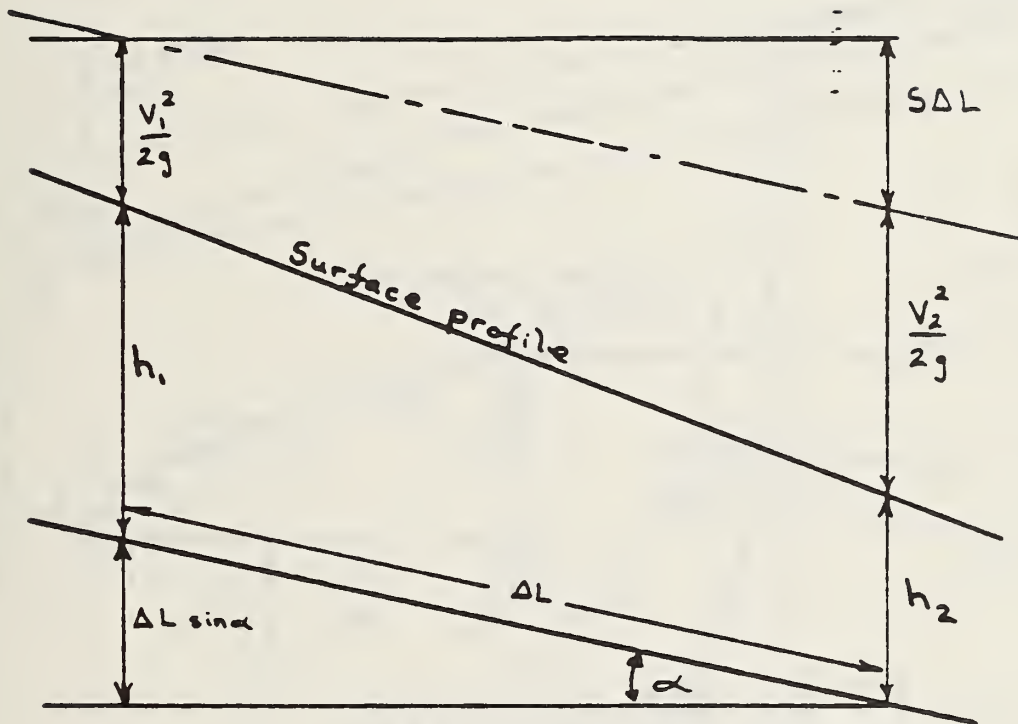
Wetted perimeter = $D \frac{\theta}{2}$

$h < D/2, \theta = 2 \tan^{-1} (\sqrt{h(D-h)} / (D/2 - h))$

$h = D/2, \theta = \pi$

$h > D/2, \theta = \pi + 2 \tan^{-1} (h - D/2) / \sqrt{h(D-h)}$

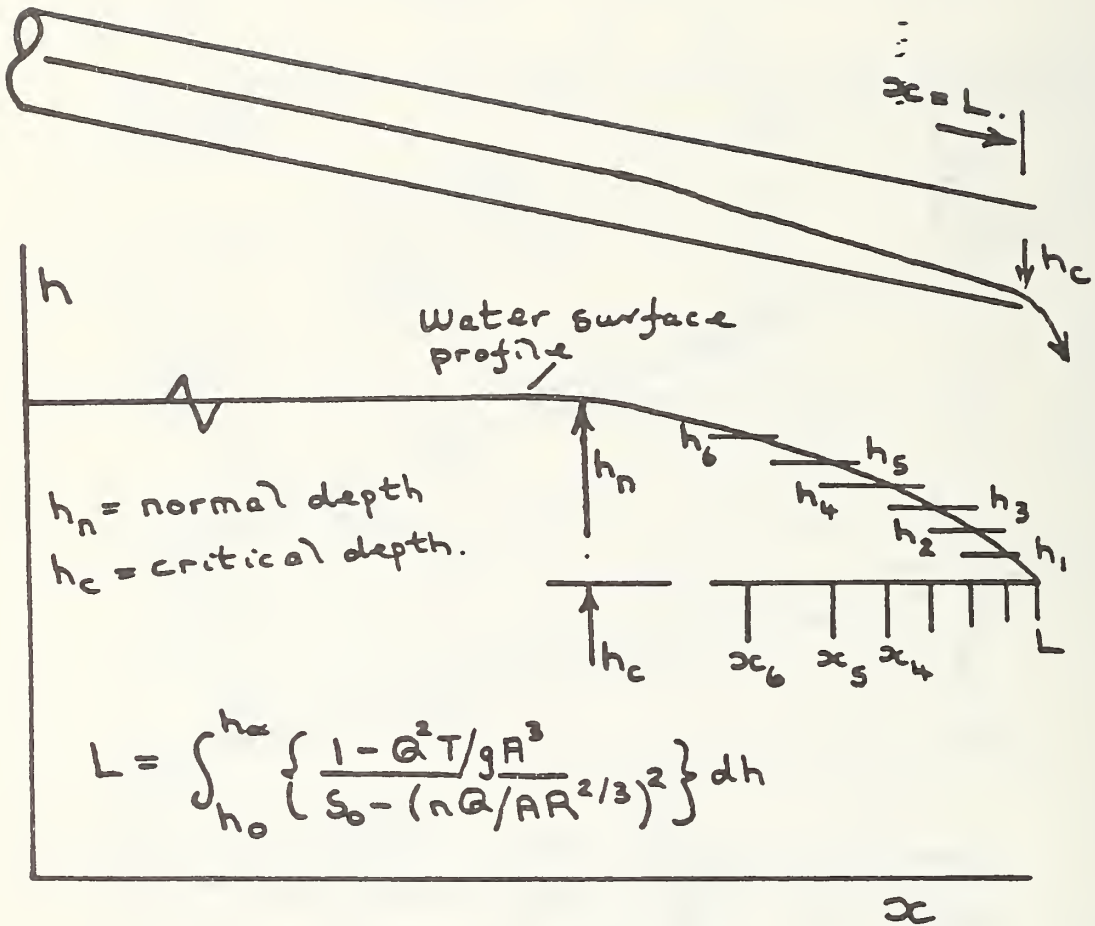
Figure 7. Summary of pipe cross section and depth dependent parameters calculations



Gradually varied flow, analysis based on head loss at any section being equal to Manning loss prediction, where

$$S = - \frac{\Delta E}{\Delta L} = \left(\frac{n Q}{A m^{2/3}} \right)^2$$

Figure 8. Basis of gradually varied flow depth prediction



- Note, i Δx increases as calculation proceeds.
- ii Calculation proceeds upstream from exit, $h = h_c$ initial condition.
- iii $\Delta h = (h_n - h_c) / n$, n in range 10-30.

Figure 9. Schematic representation of numerical integration to determine water surface profile

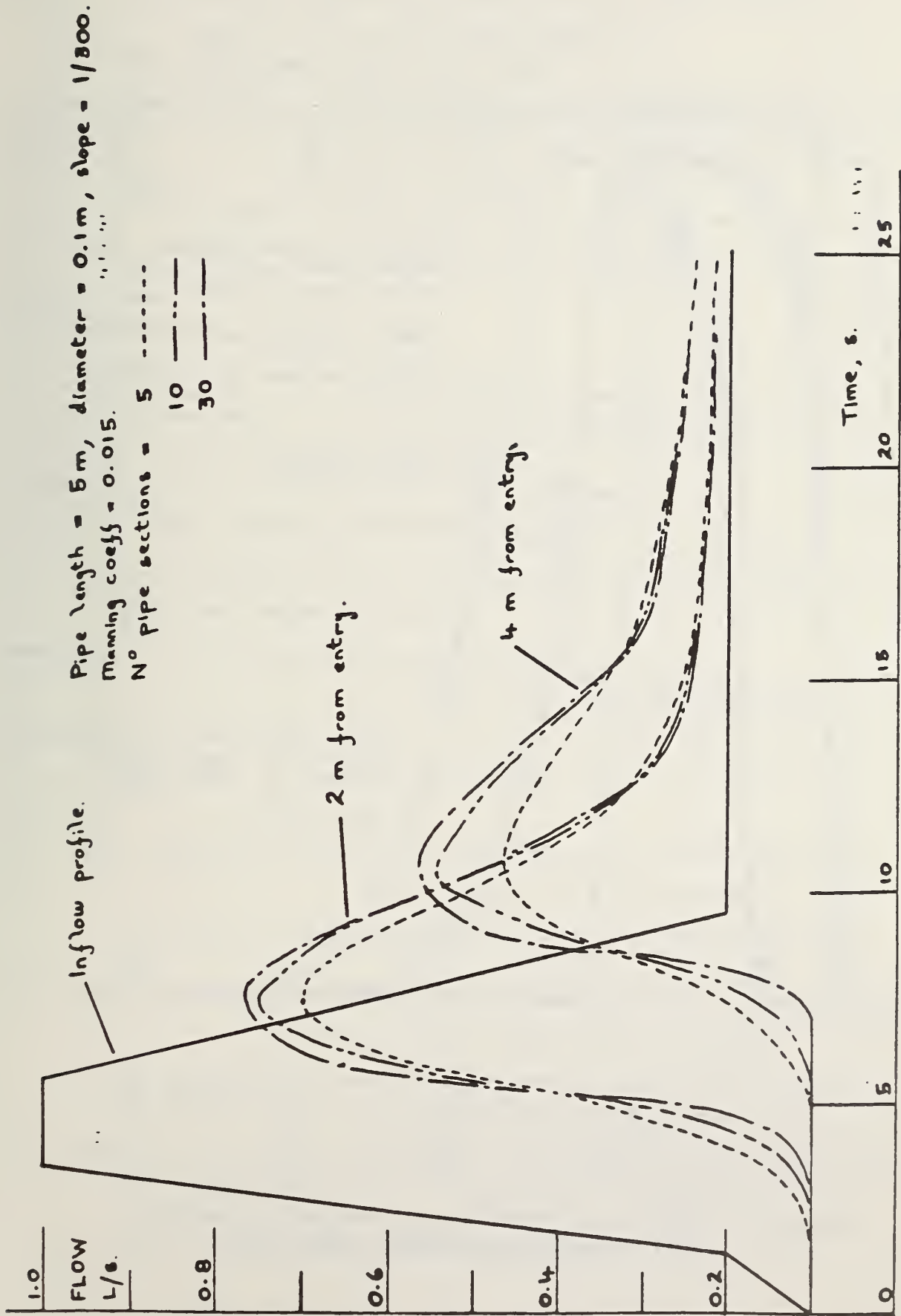


Figure 10. Influence of the choice of pipe section length on subcritical flow parameter predictions

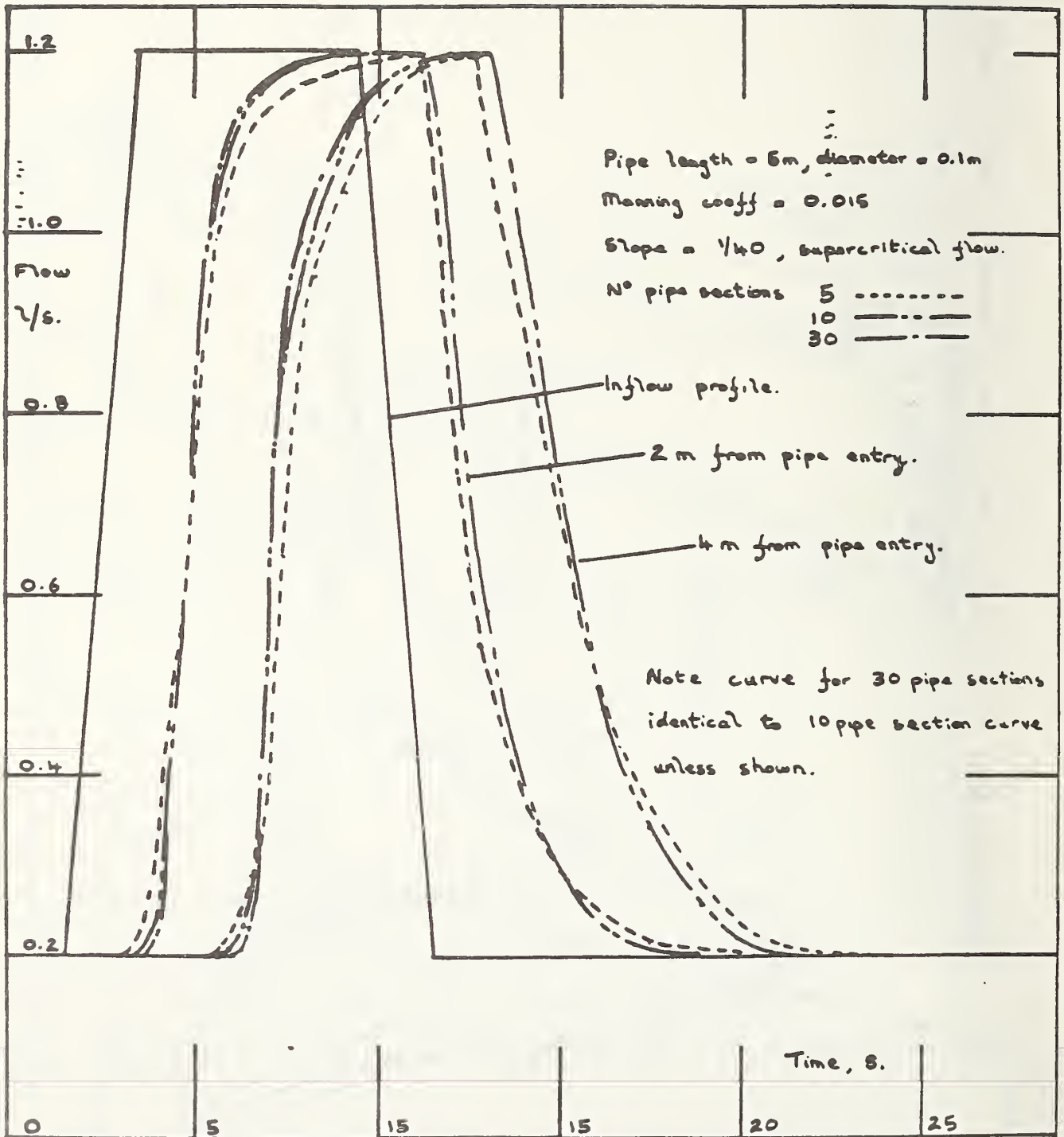


Figure 11. Influence of the choice of pipe section length on supercritical flow parameter predictions

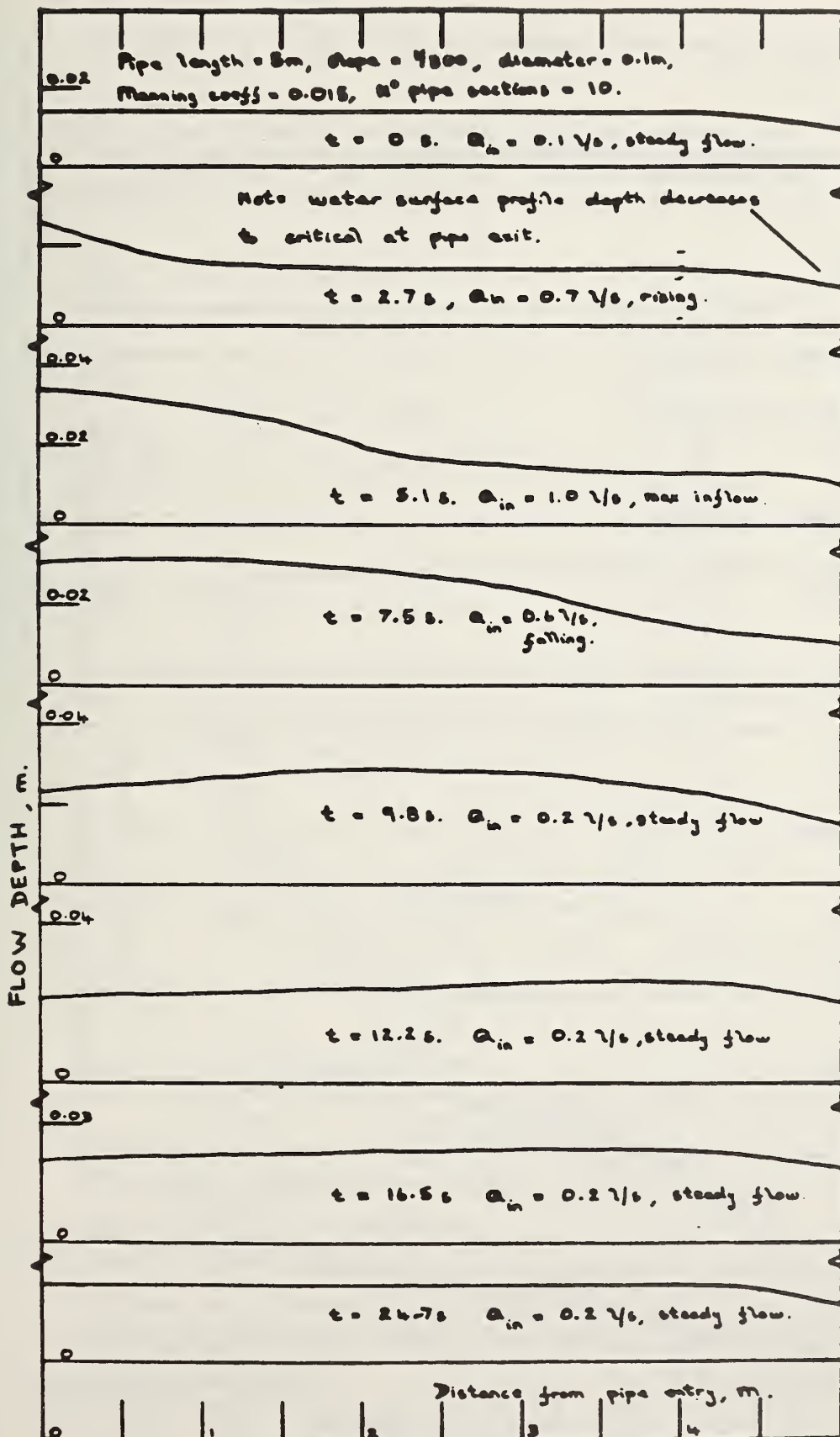


Figure 12. Depth of flow predictions for a surge introduced into subcritical flow

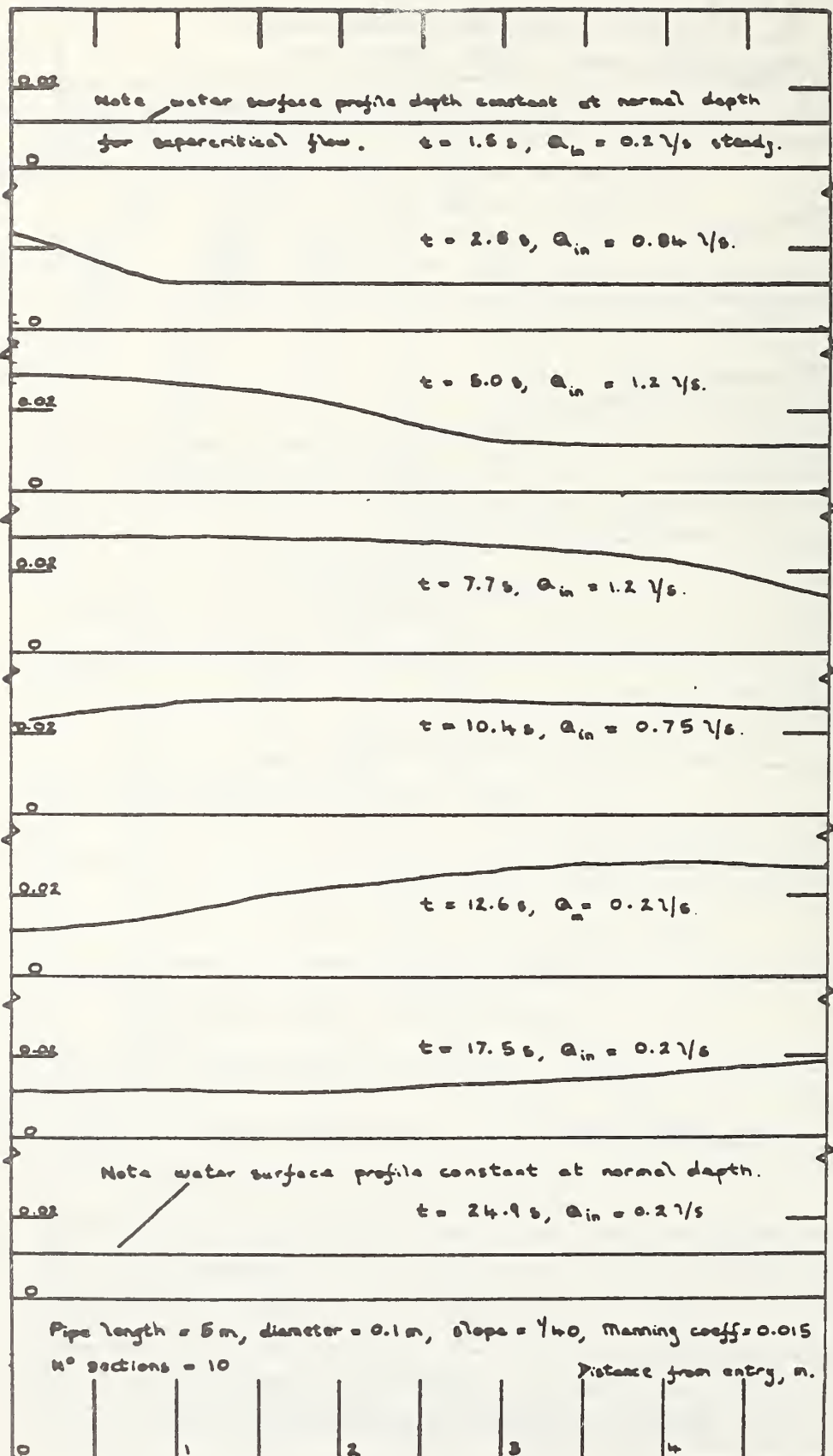


Figure 13. Depth of flow prediction for a surge introduced into supercritical flow

Pipe length = 5 m, diameter = 0.1 m

N° pipe sections = 10, Manning coeff = 0.015

Slope = 1/300

1/100

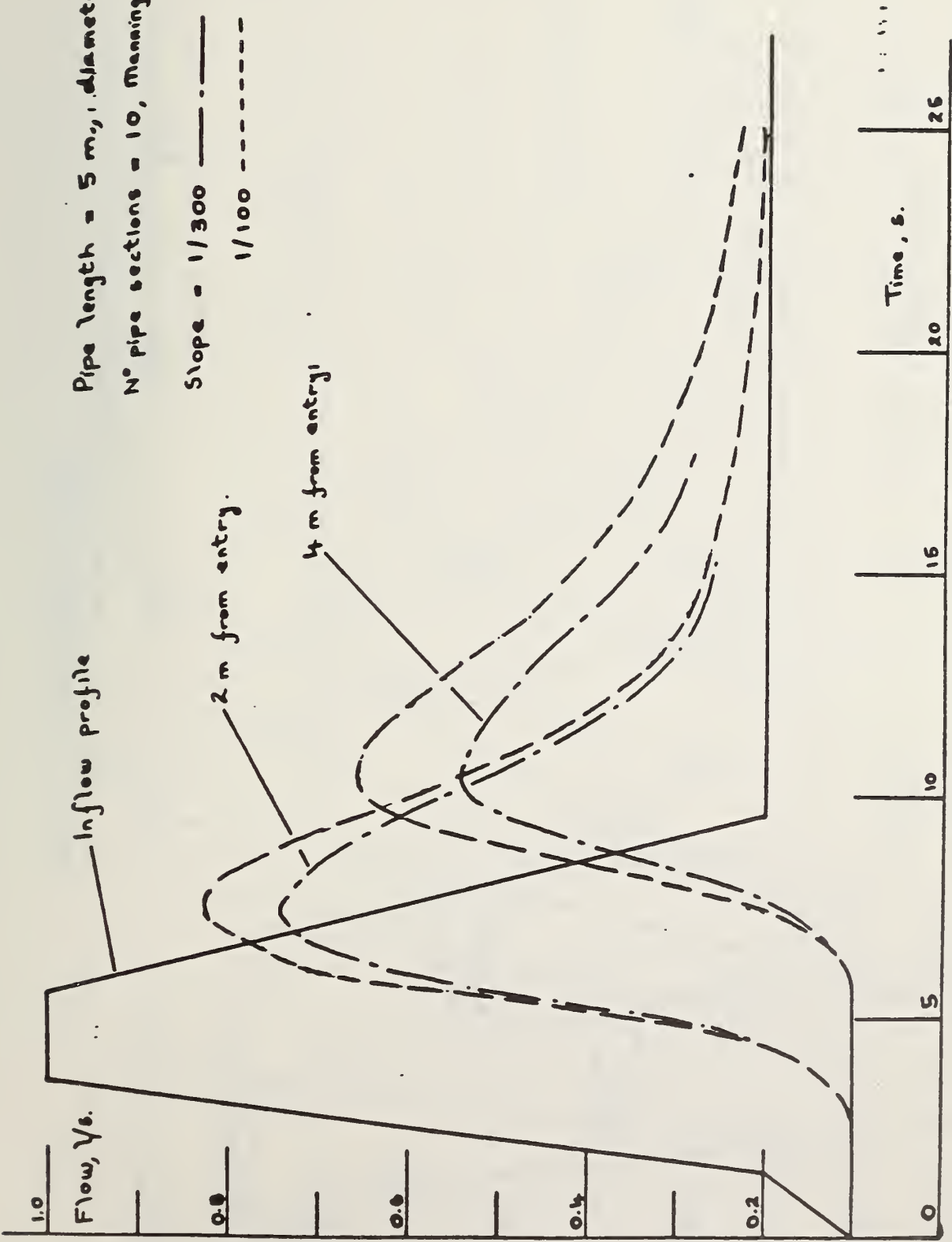


Figure 14. Comparison of surge response to a 2 s peak duration inflow at pipe gradients of 1/100 and 1/300

Pipe length = 5 m, diameter = 0.1 m, slope = 1/300
 N° pipe sections = 10.
 Manning coeff = 0.015.

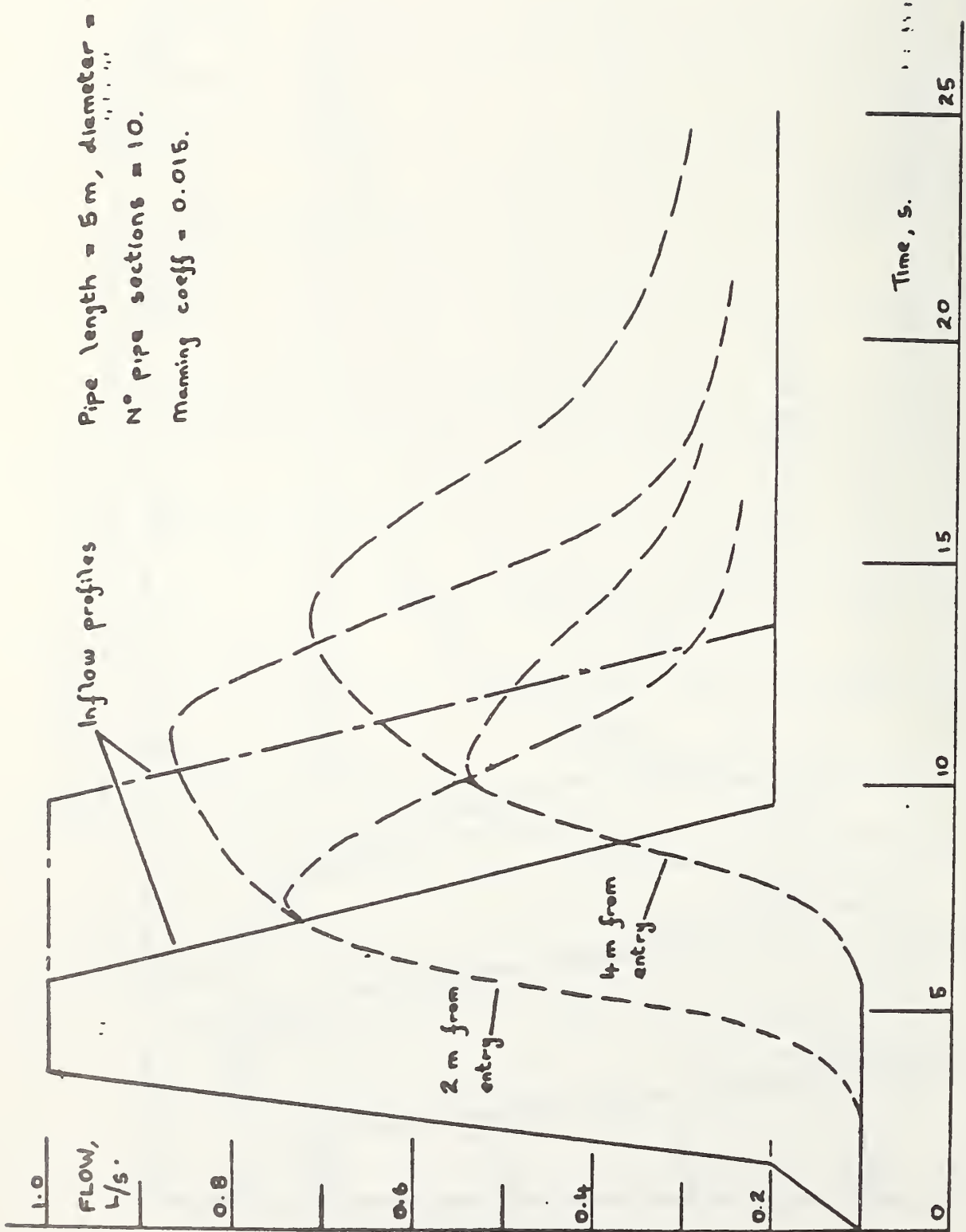


Figure 15. Comparison of surge response to a 2 s and 6 s peak inflow at a pipe gradient of 1/300

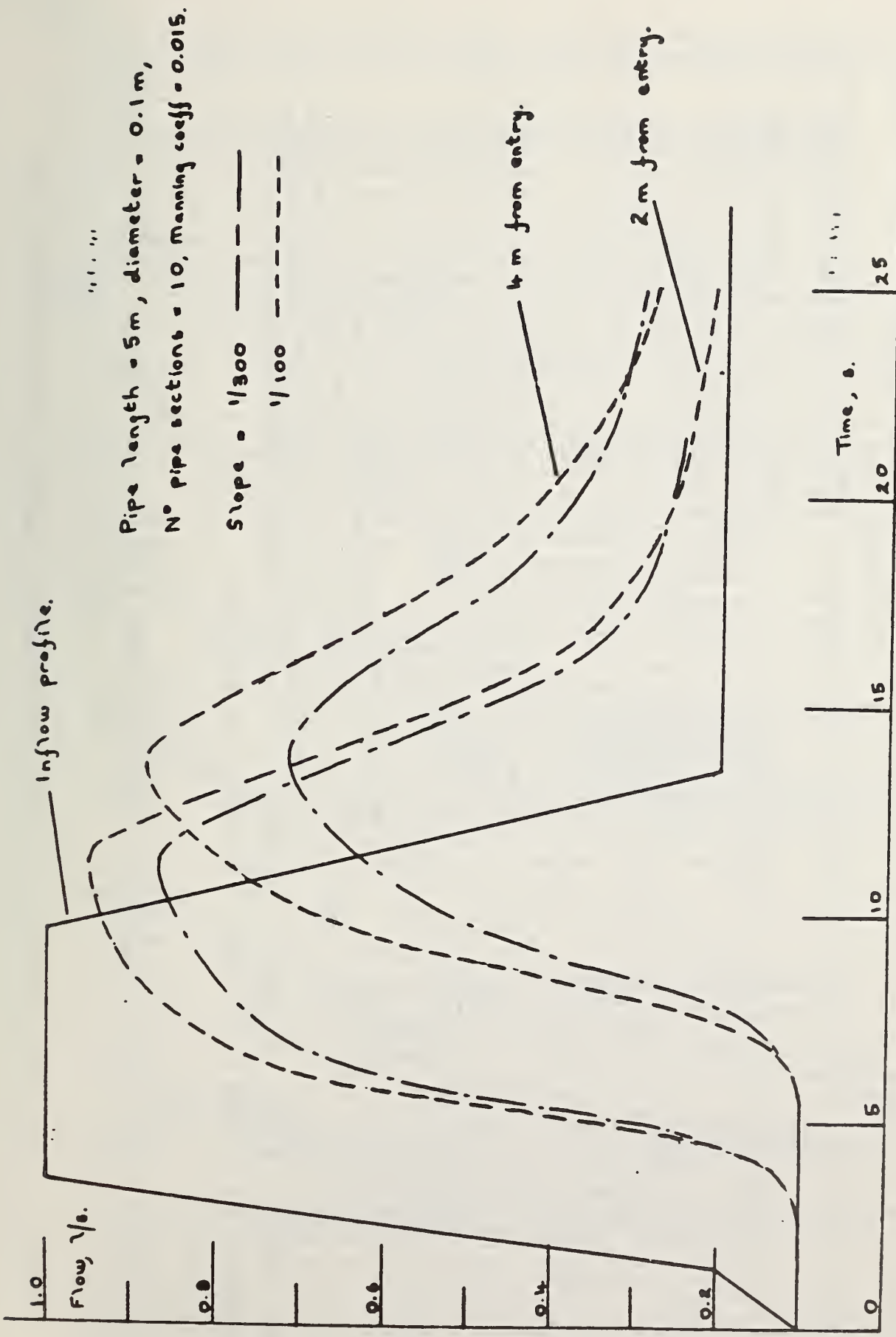


Figure 16. Comparison of surge response to a 6 s peak inflow duration at pipe gradients of 1/100 and 1/300

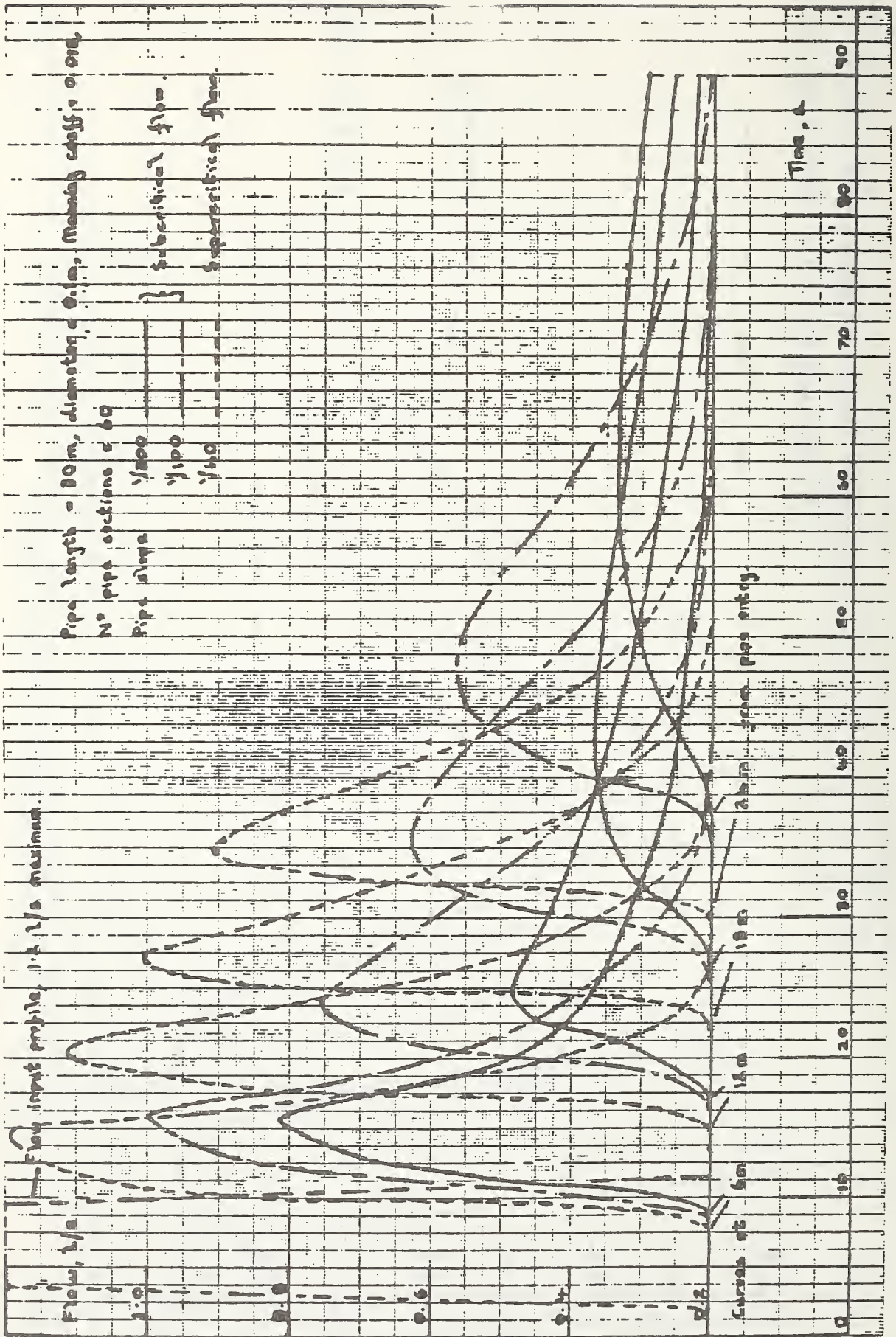


Figure 17. Flow attenuation along a 30 m pipe, 0.1 m diameter at gradients 1/40, 1/100 and 1/300

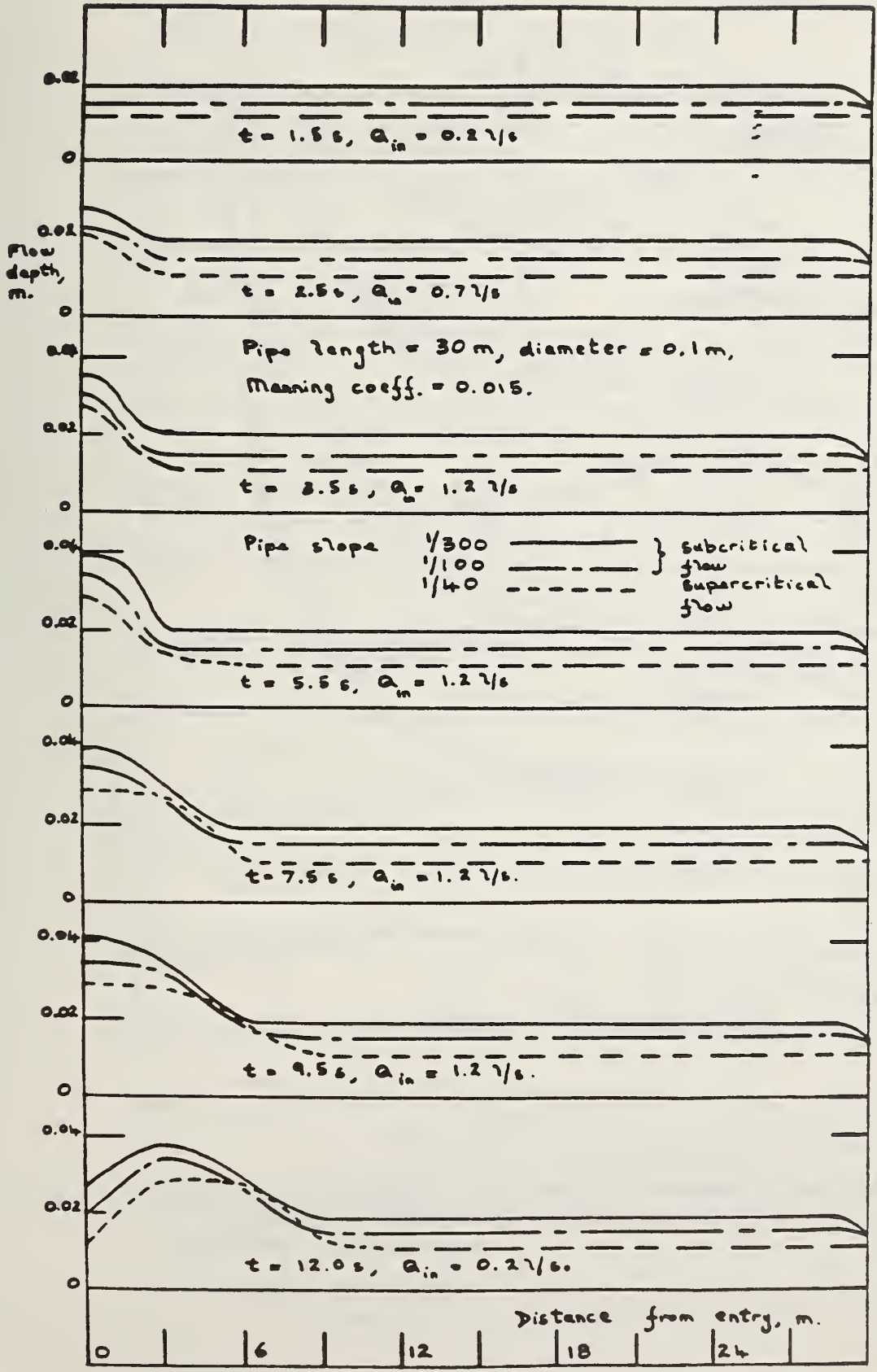


Figure 18. Flow depth predictions along a 30 m pipe at 1/400, 1/100 and 1/300 gradients in response to a 1.27 l/s peak inflow range

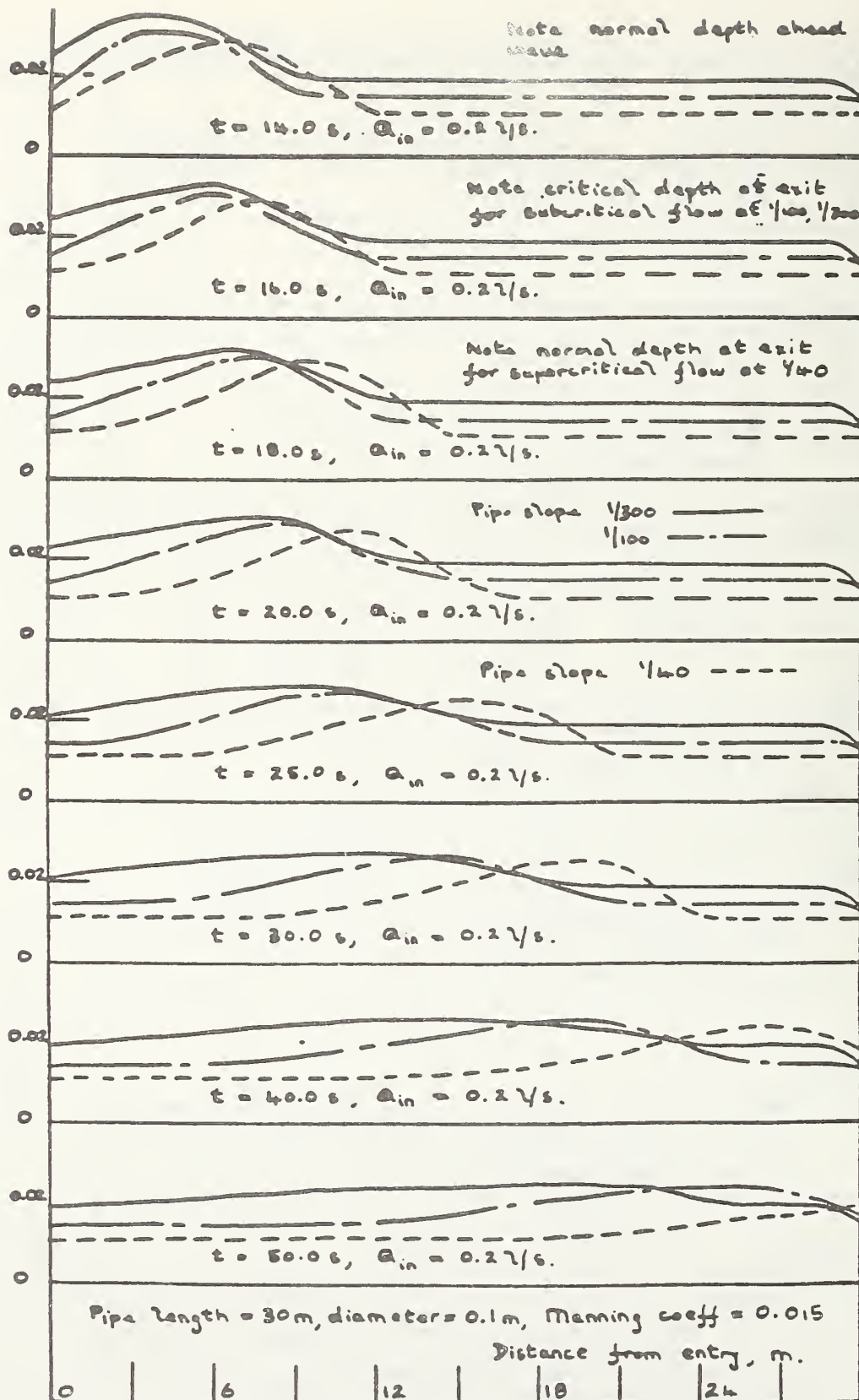


Figure 19. Continuation of figure 18

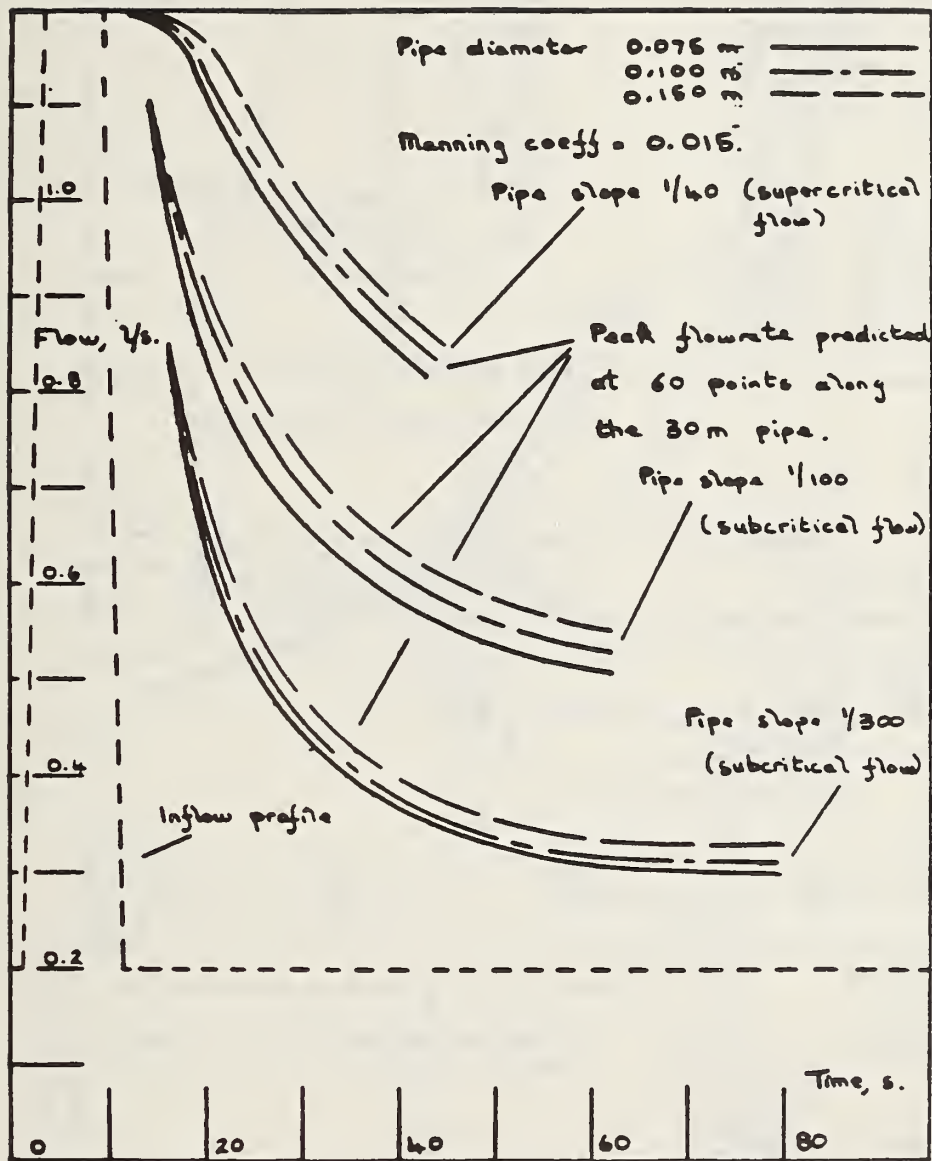


Figure 20. Peak flow rate predicted along a 30 m pipe for pipe gradients 1/400, 1/100, 1/300 and pipe diameters of 0.15, 0.1, and 0.075 m

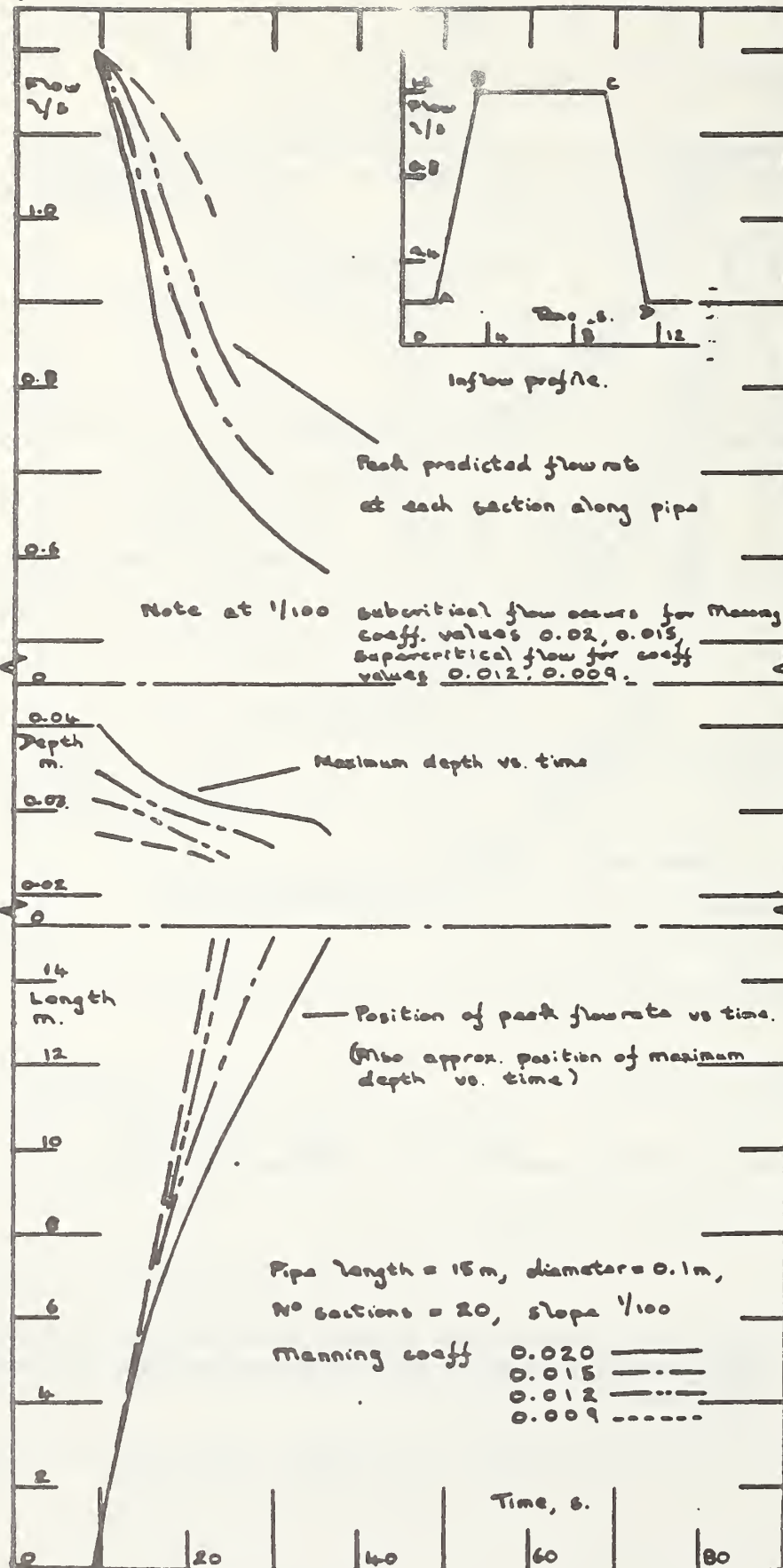


Figure 21. Peak flow rate and depth predictions along a 15 m pipe, diameter 0.1 m illustrating the dependence on roughness coefficient

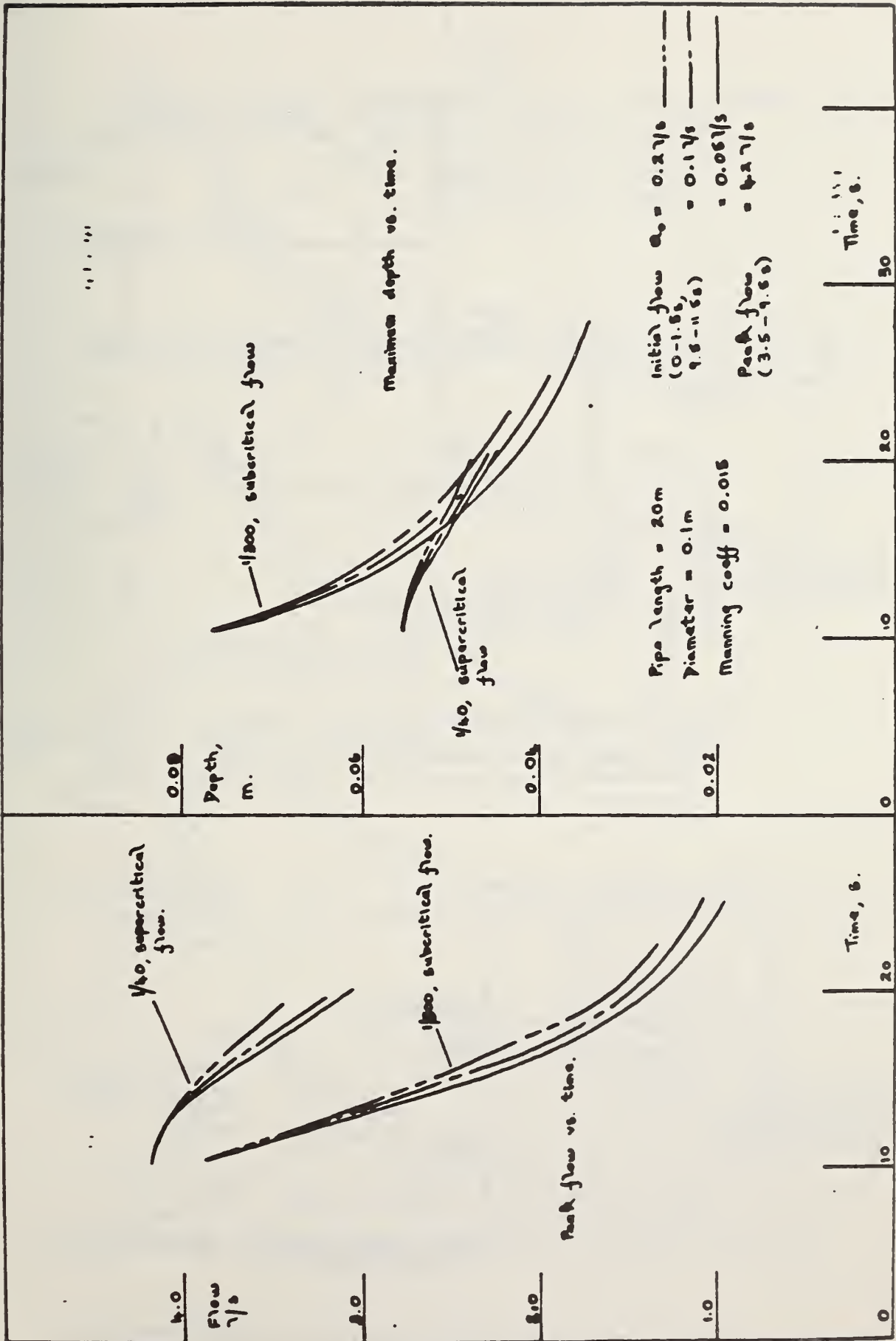


Figure 22. Effect of the initial steady flow on response to a 1.2 1/s peak range

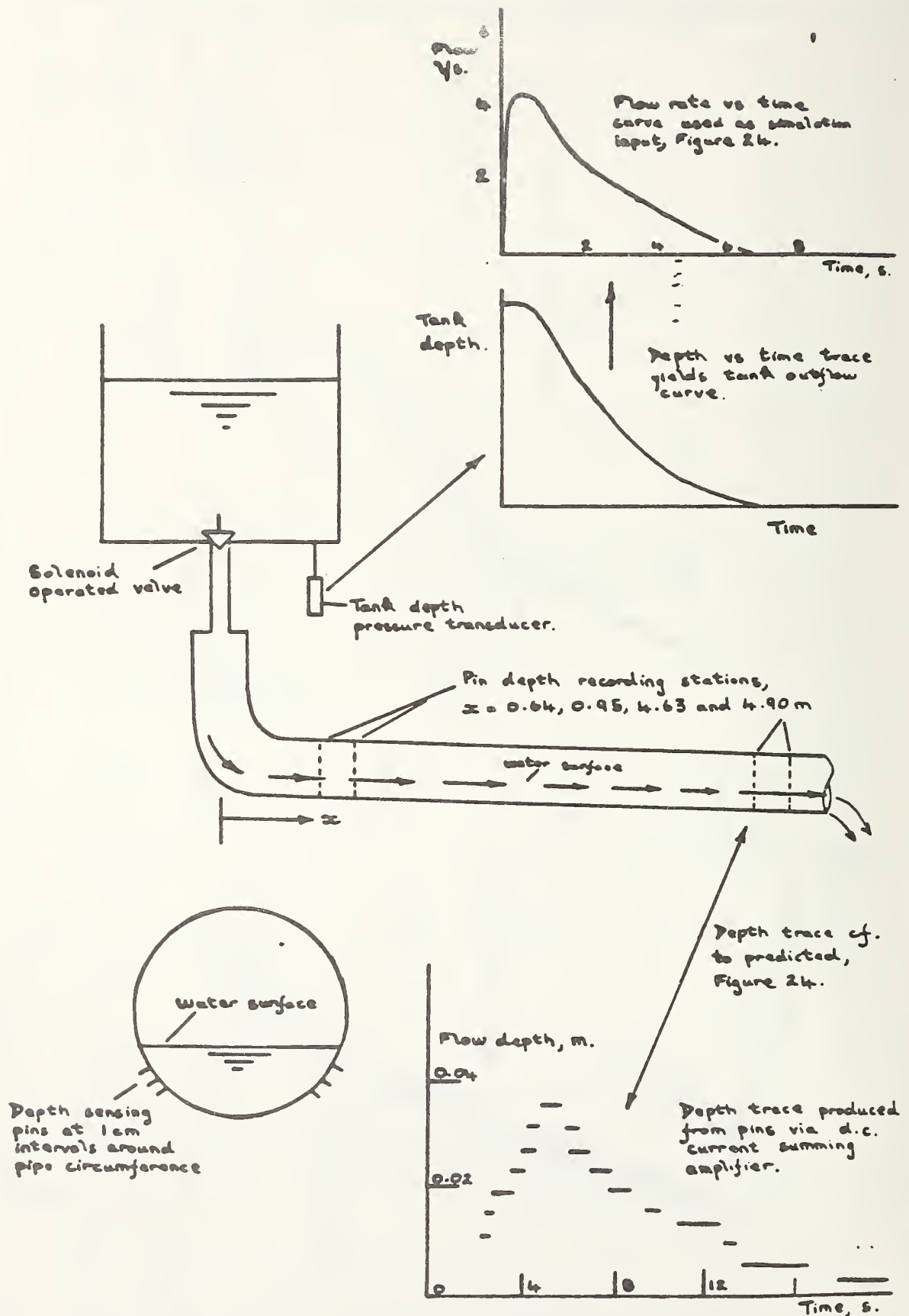


Figure 23. Summary of experimental test rig and associated inflow and depth recording instrumentation

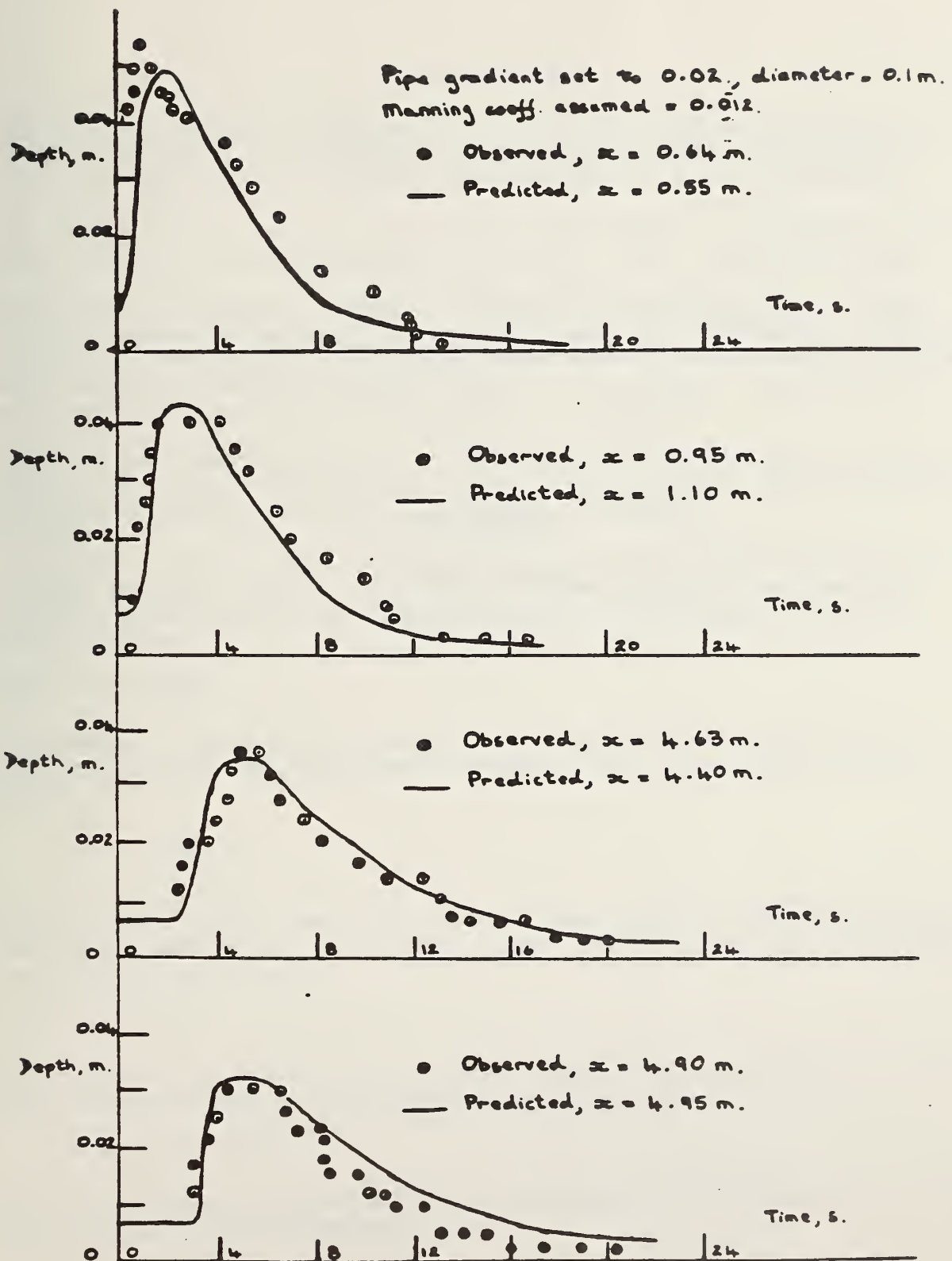


Figure 24. Comparison of observed and predicted water depth vs. time profiles

APPENDIX I

Program TRANSCC

Program TRANSCC

This appendix presents a complete print out of this program, written in Fortran, together with a flow chart and sample input data. The program was run on the NBS Center for Building Technology Perkin Elmer 732 computer.

The program accepts data in SI units with the exception of the inflow profile, this is read in as litres/second and corrected to m³/s within the program.

The program is written in terms of a series of subroutines that deal with specific aspects of the numerical solution presented in the report. In order to aid the understanding of the program each subroutine is discussed individually, with the calculation methods outlined in each case. The titles used refer to the program print out included in this appendix.

Note that the notation employed in this appendix in describing the various subroutines is compatible with that used in the main report and not the program notation, although in most cases the variation is small.

The program as written applies only to simple straight pipes with choice of constant gradient, diameter and roughness, however these subroutines can obviously be utilized in the modelling of more complex pipe networks in future programs.

Subroutine TIMINC

This subroutine determines the maximum values of wave speed and velocity at any section along the pipe at each time step. This ensures that the next time increment

$$\Delta t = \frac{\Delta x}{(V + c)}$$

is always sufficiently small to ensure a stable solution. This effectively removes the need for a time step factor, but this is retained in the program and normally set to unity.

Subroutine LOSS

This subroutine calculates the equivalent steady flow friction loss over each pipe section by means of the Manning equation, defined as

$$S = V |V| n^2/m^{4/3}$$

Note the use of V * absolute value of V to ensure that frictional forces always oppose the local flow direction.

Subroutine DEPTH

This subroutine is only called at the initial time zero to calculate the normal and critical depths based on the initial assumed flow. The values of h_c and h_n are then used to guide the solution whenever a subcritical or supercritical flow calculation choice arises.

Subroutine INFLOW

This subroutine calculates the inflow to the pipe at any time during the simulation, based on linear interpolation between successive pairs of Q, T coordinates.

Subroutine SHAPE

This subroutine calculates flow surface width, T, area A and wetted perimeter depth.

It is also used, at the initial time zero to calculate the terms necessary to provide the subcritical water surface profile.

It should be noted that this subroutine could be rewritten for any other pipe cross sectional shape and that the program in general is not restricted to circular cross section pipes. SHAPE is called from many of the other subroutines.

Subroutine WAVSPD

This subroutine namely simply local wavespeed based on

$$c = \sqrt{\frac{gA}{T}}$$

and utilizes SHAPE

Subroutine PROFIL

This subroutine is only fully employed if the initial flow is shown to be subcritical as a result of the normal and critical depths calculated via DEPTH.

The water surface profile is calculated from an assumed critical depth at pipe exit by means of the techniques described in the report. The calculation utilizes SHAPE. If the flow is supercritical then PROFIL sets all depths equal to the normal flow depth.

Subroutine INTER

This subroutine carries out the necessary interpolations to fix conditions at points R and S in subcritical flow, and R and S' in supercritical flow, figure 4 main text refers.

Subroutine ENTRY

This subroutine deals with the flow depth, velocity and wave speed at the upstream boundary. The inflow at any time is calculated from INFLOW and this flow rate is then employed, in the subcritical case, in conjunction with the appropriate C^- characteristic to yield the required parameter values, figure 5 and the section 3.3.4 of the main text.

In the supercritical flow case, identified in terms of the initial flow normal to critical flow depth comparison, the inflow curve is solved in conjunction with the normal depth relationship as the downstream conditions, represented by the C^- characteristic previously employed, can no longer effect conditions at pipe entry.

Subroutine NODAL

This subroutine solves the C^+ and C^- characteristics at all internal pipe sections between $x = \Delta x$ and $x = L - \Delta x$, figure 4 main text refers, for both sub and supercritical flow.

In addition for supercritical flow it also calculates the flow exit condition as these are based solely on upstream conditions.

Subroutine EXIT

This subroutine is only utilized for the subcritical flow case. The exit boundary conditions are determined by solution of the appropriate C^+ characteristic, figure 4 main text, with the critical depth expression

$$\frac{Q^2 T}{g A^3} - 1 = 0$$

and $Q = VA = A(X2 - X1h)$

As this is effectively a loss coefficient concentrated at pipe exit the boundary equation must be solved in the form

$$\frac{Q |Q| T}{g A^3} - 1 = 0$$

or $(X2 - X1h) |(X2 - X1h)| \frac{T}{g A} = 1$

where $| |$ indicate the absolute value of the term enclosed.

Solution is performed by means of the bisection technique described in the main text.

Subroutine ASSIGN

This subroutine reassigns the values calculated at the end of a time step, points P in figure 4 main text, to allow the calculation procedures to move on one time increment. This is necessary to avoid program storage space problems.

FLOW CHART PROGRAM TRANSCC

Set up initial conditions.

Time = 0.0

Read pipe data, diameter D, Manning coeff RM, slope $S\emptyset$, length PL.

Read calculation data, N - N° pipe sections,
TMAX - calculation duration
TFAC - time step factor

Read inflow profile, NPTS - N° of coordinate pairs
Flow - QIN, time TIN.

Adjust flow units from l/s to m³/s.

Calculation of initial steady conditions at time zero.

CALL DEPTH - calculation of normal and critical depths at initial flow.

$h_c < h_n$

$h_n < h_c$

Subcritical flow

CALL PROFIL - calculate water surface profile by gradually varied flow analysis. Interpolate to yield depth at N sections.

Supercritical flow

CALL PROFIL - set all pipe flow depths equal to normal value.

CALL ASSIGN - set up base arrays H, V, C
CALL TIMINC - identify maximum V, C
Calculate time and pipe length increments,
 $\Delta x = PL/N$
 $\Delta t = \Delta x / (TFAC \times (V + C)_{MAX})$

Output - Initial conditions and pipe description
- Table headings

- Depth, Velocity, Flow, Wavespeed at each Δx increment if $N < 10$, at 1/10 pipe length points length points if $N > 10$ and a multiple of 10.

A - Update time and commence unsteady flow simulation

CALL TIMIC - identify maximum V, C. Calculate next time increment Δt .

Time = Time + Δt

Check Time vs TMAX

Time < TMAX
Go to B

Time \geq TMAX
Go to E

B - unsteady flow calculations.

CALL INFLOW - calculate pipe inflow value

CALL INTER - interpolate to obtain base conditions HR, HS etc. Contains choice based on flow regime.

CALL LOSS - calculation of equivalent steady loss terms SR, SS.

CALL ENTRY - solves upstream boundary dependant on flow regime

CALL NODAL - solves C^+ , C^- , characteristics based on output of INTER and LOSS. For supercritical flow also calculates exist boundary conditions.

Supercritical flow, Go to C

Subcritical flow, CALL EXIT - solves exit boundary equation with C^+ characteristic

C - CALL ASSIGN - set up base arrays H, V, C.

Output - H, V, Q, C at appropriate points.

Go to A

E - END

SAMPLE INPUT DATA, PROGRAM TRANSCC

Line 1.

Pipe diameter, Manning coeff., slope, length

Format 4F10.4

▽▽▽▽ 0.1000 ▽▽▽▽ 0.0150 ▽▽▽▽ 0.0100 ▽▽▽▽ 5.000

Line 2.

N° calculation sections, Run time, Time step factor (Note: N° calculation sections either < 10 or multiple of 10 to match output format, time step factor normally set = 1.)

Format I3, 2F10.4

▽ 10 ▽▽ 200.0000 ▽▽▽▽ 1.0000

Line 3.

N° pairs of coordinates on inflow-time curve.

Format I3

▽▽ 5

Line 4 to 8.

Inflow QIN at time TIN

Format 2F10.4

▽▽▽▽ 0.0500 ▽▽▽▽ 0.0000

▽▽▽▽ 2.5000 ▽▽▽▽ 1.0000

▽▽▽▽ 2.5000 ▽▽▽ 10.0000

▽▽▽▽ 0.0100 ▽▽▽ 12.5000

▽▽▽▽ 0.0100 ▽▽ 200.0000

Units - SI units used in data fields except for inflow QIN in m^3/s , converted to m^3/s in program output in SI, except flow rate in m^3/s .

SBATCH

C TRANSC ARE A SERIES OF PROGRAMS DESIGNED TO APPLY THE METHOD OF
C CHARACTERISTICS SOLUTION TO THE EQUATIONS DEFINING
C UNSTEADY FLOW IN PARTIALLY FILLED CHANNELS.
C
C

DIMENSION GP(61),QIN(30),TIN(30),VP(61),HP(61),CP(61)
DIMENSION V(61),H(61)
DIMENSION VF(61),HR(61),CF(61),VS(61),HS(61),CS(61),SS(61)
DIMENSION SR(61),XR(61),XS(61),XM(61),C(61)
COMMON/CM1/CTO,DT,DX,D,SO,PL,SEC,XK,RM
COMMON/CM2/N,TMAX
COMMON/CM3/NPTS,QIN,TIN
COMMON/CM4/V,H,C,V²,HR,CR,XR,SP,VS,HS,CS,XS,SS,XN
COMMON/CM5/HC,HN
COMMON/CM6/OP,VP,HP,CP
COMMON/CM7/CL

C
C
C
C
C
C
C

SET INITIAL CONDITIONS

TIME=C.0

C READ PIPE DESCRIPTION DATA

READ(4,100)D,RM,SO,PL

C D-DIA. RM-MANNING COEFF. SO-PIPE SLOPE. PL-PIPE LENGTH
100 FORMAT(4F10.4)

C READ CALCULATION DATA

READ(4,103)N,TMAX,TFAC

IF(N.LE.10) N2=1

IF(N.GT.10) N2=N/10

C N2 INCREMENT BETWEEN OUTPUT NODES,ALLOWS MORE THAN 10
C CALCULATION NODES TO BE USED.

C N-NUMBER OF PIPE SECTIONS CONSIDERED, TMAX-DURATION OF CALC.
C TFAC-TIME STEP FACTOR,1-10.

103 FORMAT(13,2F10.4)

C READ INFLOW DATA PROFILE. INFLOW PROFILE USED IS BASED ON
C A LINEAR INTERPOLATION BETWEEN THESE DATA POINTS. NOTE DATA
C READ IN IN L/S BUT USED IN PROGRAM IN M³/S.

READ(4,102)NPTS

102 FORMAT(13)

DO 50 I=1,NPTS

READ(4,104)QIN(I),TIN(I)

104 FORMAT(2F10.4)

QIN(I)=QIN(I)/1000.0

50 CONTINUE

C
C
C
C
C

C CALCULATION OF INITIAL CONDITIONS ALONG THE PIPE
C BASED ON GRADUALLY VARIED FLOW EQUATIONS. THE
C TERMINAL CONDITIONS IN THE PIPE ARE BASED ON
C CRITICAL DEPTH AT PIPE EXIT.

CALL DEPTH(TIPE)

CALL PROFIL(QIN(1),HN,HC,XN)

CALL ASSIGN(N)

C CALCULATION OF TIME STEP AND LENGTH SECTION.

CALL TIMINC(N,VP,CP,VN,CN)


```

C     THIS SUBROUTINE CALCULATES FLOW AREA, SURFACE WIDTH AND
C     WETTED PERIMETER BASED ON FLOW DEPTH
C     THIS SUBROUTINE ALSO CALCULATES WATER SURFACE PROFILE
C     AND SETS UP BASE CONDITIONS ALONG THE PIPE AT TIME ZERO.
      R=D/2.0
      PI=3.142
      IF(H.LT.R)THETA=2.0*ATAN(SQRT(H*(D-H))/(R-H))
      IF(H.EQ.R)THETA=PI
      IF(H.GT.R)THETA=PI+2.0*ATAN((H-R)/(SQRT(H*(D-H))))
      A=((D**2)/8.0)*(THETA-SIN(THETA))
      PER=D*THETA/2.0
      T=2.0*((H*(D-H))**0.5)
      IF(TIME.GT.C.0) GOTO 1
      Q=QIN(1)
      G=9.81
      CON=RM**2/SC
      HCRIT=1.0-(C**2)*T/(G*A**3)
      HNRHM=1.0-(C**2)*CON/((A**3.333)/(PER**1.333))
      DL=HCRIT/(HNRHM**50)
1     CONTINUE
      RETURN
      END

C
C
C
C
C
C
      SUBROUTINE WAVSPD(H,C)
C     THIS SUBROUTINE CALCULATES WAVE SPEED BASED ON DEPTH AND CROSS
C     SECTION SHAPE.
      CALL SHAPE(TIME,H,AREA,T,PER)
      C=SQRT(9.81*AREA/T)
      RETURN
      END

C
C
C
C
      SUBROUTINE PROFIL(C,HN,HC,XN)
C     THIS SUBROUTINE CALCULATES THE INITIAL WATER SURFACE
C     PROFILE BASED ON CRITICAL DEPTH AT PIPE EXIT.
      DIMENSION HP(61),VP(61),QP(61),CP(61)
      DIMENSION X(30),DEP(30),XN(61)
      DIMENSION X1(30),DEP1(30)
      COMMON/CH1/DT0,DT,DX,D,SO,PL,SEC,XK,RM
      COMMON/CH2/N,TMAX
      COMMON/CH6/CP,VP,HP,CP
      COMMON/CH7/CL

      IF(HN.LE.HC) GOTO 900
      DH=(HN-HC)/30.0
      IS=1
      H1=HC
      CALL SHAPE(TIME,H1,A,T,PER)
      X(1)=PL
      DEP(1)=HC
      SL=0.0
C     WATER SURFACE PROFILE CALCULATIONS.
      DO 80 I=1,200,2
      IS=IS+1
      H2=HC+DH*FLOAT(I+1)
      H3=HC+DH*FLOAT(I)

```

```

CALL SHAPE(TIME,H1,A,T,PEF)
DL1=DL
CALL SHAPE(TIME,H2,A,T,PER)
DL2=DL
CALL SHAPE(TIME,H3,A,T,PEF)
DL3=DL
DXP=DH*(DL1+DL2+4.C*DL3)/3.0
SL=SL-DXP
H1=H2
IF(SL.GE.PL) GOTO 81
X(IS)=PL-SL
IF(H1.GE.FN) GOTO 93
DEP(IS)=H1
80 CONTINUE
81 X(IS)=0.0
NIS=IS
IF(H1.GE.FN) GOTO 93
DEP(IS)=H1
GOTO 84
83 DEP(IS)=HN
GOTO 84
84 IF(X(IS).GT.0.0) GOTO 85
GOTO 86
85 X(IS+1)=0.0
DEP(IS+1)=FN
NIS=IS+1
86 CONTINUE
C
C
C INTERPOLATION REQUIRED TO DETERMINE DEPTH AT EACH NODE.
900 CONTINUE
DX=PL/FLOAT(N)
XN(1)=0.0
DO 87 I=2,N+1
XN(I)=XN(I-1)+DX
87 CONTINUE
IF(HN.LE.FC) GOTO 901
N2=NIS+1
DO 94 J=1,NIS
N2=N2-1
X1(J)=X(N2)
DEP1(J)=DEP(N2)
WRITE(3,93)X1(J),DEP1(J)
93 FORMAT(10X,2F10.5)
94 CONTINUE
DO 95 J=1,NIS
X(J)=X1(J)
DEP(J)=DEP1(J)
95 CONTINUE
HP(1)=DEP(1)
HP(N+1)=HC
DO 88 I=2,N
DO 89 K=1,NIS-1
IF(XN(I).GT.X(K).AND.XN(I).LE.X(K+1)) GOTO 90
89 CONTINUE
90 HP(I)=DEP(K)+(DEP(K+1)-DEP(K))*(XN(I)-X(K))/(X(K+1)-X(K))
88 CONTINUE
C SET UP BASE CONDITIONS AT TIME ZERO.
901 CONTINUE
DO 91 I=1,N+1
IF(HN.LE.FC) HP(I)=HN
CALL SHAPE(TIME,HP(I),A,T,PEF)
VP(I)=0/A

```

```

JP(I)=0*1000.C
CALL WAVSPD(HP(I),CP(I))
CONTINUE
RETURN
END

```

91

C
C
C
C
C
C
C

```

SUBROUTINE INTER(N)
DIMENSION V(61),H(61),C(61),VR(61),HR(61),CR(61),VS(61)
DIMENSION HS(61),CS(61),SP(61),SS(61),XM(61)
DIMENSION XS(61),XR(61)
COMMON/CH1/CTO,DT,DX,D,SO,PL,SEC,XK,RM
COMMON/CH4/V,H,C,VR,HR,CR,XR,SP,VS,HS,CS,XS,SS,XM
COMMON/CH5/FC,FM

```

THIS SUBROUTINE SETS UP, BY INTERPOLATION, THE BASE CONDITIONS FOR THE NEXT TIME STEP.

C
C
C

```

THETA=DT/DX
N1=N+1
DO 1 I=2,N1
VR(I)=(V(I)+THETA*(C(I)*V(I-1)-V(I)*C(I-1)))
1 / (1.0+THETA*(V(I)-V(I-1)+C(I)-C(I-1)))
CR(I)=(C(I)*(1.0-VR(I)*THETA)+C(I-1)*VR(I)*THETA)
1 / (1.0+C(I)*THETA-C(I-1)*THETA)
HR(I)=H(I)-(H(I)-H(I-1))*THETA*(VR(I)+CR(I))
XR(I)=XM(I)-(VR(I)+CR(I))*DT

```

1

```

CONTINUE
IF(FM.LE.FC) GOTO 4
DO 2 I=1,N
VS(I)=(V(I)-THETA*(V(I)*C(I+1)-C(I)*V(I+1)))
1 / (1.0-THETA*(V(I)-V(I+1)-C(I)+C(I+1)))
CS(I)=(C(I)+VS(I)*THETA*(C(I)-C(I+1)))
1 / (1.0+THETA*(C(I)-C(I+1)))
HS(I)=H(I)+THETA*(VS(I)-CS(I))*(H(I)-H(I+1))
XS(I)=XM(I)+(VS(I)-CS(I))*DT

```

2

```

CONTINUE
GOTO 3

```

4

```

DO 5 I=2,N+1
VS(I)=(V(I)*(1.0+THETA*C(I-1))-V(I-1)*THETA*C(I))/
1 (1.0+THETA*(V(I)-V(I-1)+C(I-1)-C(I)))
CS(I)=(C(I)+VS(I)*(C(I)-C(I-1)))/(1.0+THETA*(C(I-1)-C(I)))
HS(I)=H(I)-(H(I)-H(I-1))*THETA*(VS(I)-CS(I))

```

5

CONTINUE

3

CONTINUE

RETURN

END

C
C
C
C
C
C
C

```

SUBROUTINE ENTRY(TIME)

```

THIS SUBROUTINE CALCULATES THE UPSTREAM BOUNDARY CONDITIONS AT EACH TIME STEP BASED ON A KNOWN INFLOW PROFILE.

```

DIMENSION OP(61),CIN(30),TIM(30),VP(61),HP(61),CP(61)

```

C
C

```

DIMENSION V(61),H(61)
DIMENSION VF(61),HR(61),CR(61),VS(61),HS(61),CS(61),SS(61)
DIMENSION SF(61),XR(61),XS(61),XN(61),C(61)
COMMON/CM1/DTO,DT,DX,D,SO,PL,SFO,XK,K1
COMMON/CM2/N,TRAX
COMMON/CM3/NPTS,GIN,TIN
COMMON/CM4/V,F,C,VR,HR,CR,XR,SF,VS,HS,CS,XS,SS,XN
COMMON/CM5/FC,HN
COMMON/CM6/CP,VP,MP,CP

```

```

C
G=9.81
CON=RM**2/SC
IF(TIME.GT.C.0)CALL INFLOW(TIME,C)
IF(TIME.GT.0.0) GOTO 500
IF(TIME.EC.C.0)Q=GIN(1)
C
CALCULATION OF CRITICAL DEPTH.
UP=0
DN=0.0
HC=(UP+DN)/2.0
7
CONTINUE
CALL SHAPE(TIME,HC,AREA,T,PER)
HCRIT=1.0-(C**2)*T/(G*AREA**3)
IF(HCRIT)3,4,5
3
DN=HC
GOTO 6
5
UP=HC
6
HCN=(UP+DN)/2.0
IF(ABS((HCN-HC)/HC).LE.C.C01) GOTO 8
HC=HCN
GOTO 7
8
HC=HCN
4
CONTINUE
C
CALCULATION OF NORMAL DEPTH.
UP=0
DN=0.0
HN=(UP+DN)/2.0
9
CONTINUE
CALL SHAPE(TIME,HN,AREA,T,PER)
HNORM=1.0-(C**2)*CJN/((AREA**3.333)/(PER**1.333))
IF(HNCRM)10,11,12
10
DN=HN
GOTO 13
12
JP=HN
13
HNN=(UP+DN)/2.0
IF(ABS((HNN-HN)/HN).LE.0.C01) GOTO 14
HN=HNN
GOTO 9
14
HN=HNN
11
CONTINUE
IF(TIME.EC.C.0) GOTO 500
C
C
C
C
CALCULATION OF BOUNDARY DEPTH.
600
CONTINUE
IF(HN.LE.FC) GOTO 700
UP=0
DN=0.0
HB=(UP+DN)/2.0
15
CONTINUE
CALL SHAPE(TIME,HB,AREA,T,PER)
X3=G/CS(1)
X4=VS(1)-G*(SS(1)-S0)*DT-X3*HS(1)

```

```

MFLOW=Q-(X4+X3*HB)*AREA
IF(MFLOW)16,17,18
16 UP=HB
GOTO 19
18 DN=HB
19 HBB=(UP+DN)/2.0
IF(ABS((HBB-HB)/HB).LE.0.001) GOTO 20
HB=HBB
GOTO 15
20 HB=HBB
17 CONTINUE
MP(1)=HB
VP(1)=X4+X3*MP(1)
CALL SHAPE(TIME,H3,AREA,T,PEK)
QP(1)=AREA*VP(1)*1000.0
CP(1)=SORT(G*AREA/T)
500 CONTINUE
GOTO 800
700 CONTINUE
C CALCULATION OF NORMAL DEPTH.
UP=D
DN=0.0
HB=(UP+DN)/2.0
79 CONTINUE
CALL SHAPE(TIME,H3,AREA,T,PEK)
HNORM=1.0-(C**2)*CON/((AREA**3.333)/(PER**1.333))
IF(HNORM)80,81,82
80 DN=HB
GOTO 83
82 UP=HB
33 HBB=(UP+DN)/2.0
IF(ABS((HBB-HB)/HB).LE.0.001) GOTO 84
HB=HBB
GOTO 79
34 HB=HBB
91 CONTINUE
MP(1)=HB
CALL SHAPE(TIME,H3,AREA,T,PEK)
VP(1)=Q/AREA
QP(1)=Q*1000.0
CP(1)=SORT(G*AREA/T)
800 CONTINUE
RETURN
END

C
C
C
C
C
C
C
SUBROUTINE NDCAL(N)
DIMENSION QP(61),QIN(30),TIN(30),VP(61),HP(61),CP(61)
DIMENSION V(61),H(61)
DIMENSION VR(61),HR(61),CR(61),VS(61),HS(61),CS(61),SS(61)
DIMENSION SR(61),XR(61),XS(61),XN(61),C(61)
COMMON/CM1/DTC,DT,CX,D,SO,PL,SEC,XX,R1
COMMON/CM3/NPTS,CIN,TIN
COMMON/CM4/V,H,C,VR,HR,CR,XR,SR,VS,HS,CS,XS,SS,XN
COMMON/CM5/FC,FM
COMMON/CM6/CP,VP,HP,CP
C THIS SUBROUTINE CALCULATES THE FLOW VELOCITY AND DEPTH
C AND WAVE SPEED AT EACH OF THE NODES BETWEEN THE UPSTREAM
C AND DOWNSTREAM BOUNDARIES BY SOLUTION OF THE TWO WAVE

```

```

C      EQUATIONS.
      G=9.81
      NZ=N
      IF(MN.LE.MC) NZ=N+1
      DO 1 I=2,NZ
      X1=G/CP(I)
      X3=G/CS(I)
      X2=X1*HR(I)+VR(I)-G*(SR(I)-SC)*CT
      X4=VS(I)-X3*HS(I)-G*(SS(I)-SO)*DT
      HP(I)=(X2-X4)/(X1+X3)
      VP(I)=X4+X3*HP(I)
      CALL WAVSPD(HP(I),CP(I))
      CALL SHAPE(TIME,HP(I),X1,X3,X4)
      QP(I)=X1*VP(I)*1000.0
1     CONTINUE
      RETURN
      END

```

C
C
C
C
C
C

```

SUBROUTINE EXIT(TIME)
DIMENSION QP(61),VP(61),HP(61),CP(61)
DIMENSION V(61),H(61)
DIMENSION VR(61),HR(61),CR(61),VS(61),HS(61),CS(61),SS(61)
DIMENSION SF(61),XR(61),XS(61),XN(61),C(61)
COMMON/CM1/DT0,DT,DX,D,SG,PL,SEC,XK,R4
COMMON/CM2/N,THAX
COMMON/CM5/FC,FM
COMMON/CM4/V,H,C,VR,HR,CR,XF,SP,VS,HS,CS,XS,SS,XN
COMMON/CM6/QP,VP,HP,CP

```

C
C
C
C
C
C

THIS SUBROUTINE CALCULATES THE FLOW DEPTH AT PIPE DISCHARGE
BASED ON THE ASSUMPTION OF CRITICAL DEPTH AT SUCH A BOUNDARY.

```

      G=9.81
      X1=G/CR(N+1)
      X2=X1*HR(N+1)+VR(N+1)-G*(SF(N+1)-SO)*DT
      UP=0
      DN=0.0
      HB=(UP+DN)/2.0
5     CALL SHAPE(TIME,HB,A,T,PER)
      HEXIT=1.0-(ABS(X2-X1*HB)*(X2-X1*HB))*T/(G*A)
      IF(HEXIT)1,2,3
1     DN=HB
      GOTO 4
3     UP=HB
      GOTO 4
4     HBB=(UP+DN)/2.0
      IF(ABS((HBB-HB)/HB).LT.0.00001) GOTO 2
      HB=HBB
      GOTO 5
2     CONTINUE
      VP(N+1)=X2-X1*HB
      HP(N+1)=HB
      CALL SHAPE(TIME,HB,A,T,PER)
      CALL WAVSPD(HB,CP(N+1))
      QP(N+1)=1000.0*A*VP(N+1)
      WRITE(3,7)HP(N+1),VP(N+1),CP(N+1),CP(N+1)

```

```

7      FORMAT(/10X,'H=',E14.6,5X,'V=',E14.6,/,10X,'U=',E14.6,5X,'C=',
1 E14.6,/)
      RETURN
      END

```

```

C
C
C
C
C

```

```

SUBROUTINE ASSIGN(N)
THIS SUBROUTINE SETS UP THE NEW BASE CONDITIONS -ALONG THE
PIPE IN PREPARATION FOR THE NEXT TIME STEP.
DIMENSION CP(61),QIN(30),TIN(30),VP(61),HP(61),CP(61)
DIMENSION V(61),H(61)
DIMENSION VF(61),HR(61),CR(61),VS(61),HS(61),CS(61),SS(61)
DIMENSION SF(61),XR(61),XS(61),XN(61),C(61)
COMMON/CM3/NPTS,QIN,TIN
COMMON/CM4/V,H,C,VR,TR,CR,XR,SF,VS,HS,CS,XS,SS,XN
COMMON/CM6/CF,VP,HP,CP
DO 1 I=1,N+1
V(I)=VP(I)
H(I)=HP(I)
C(I)=CP(I)
1 CONTINUE
RETURN
END

```

```

$BEND

```

APPENDIX II
Typical Output Program TRANSCC

TEST PIPE CALCULATIONS:-
 DIAMETER = 0.1000 M.
 PIPE SLOPE = 0.0100

MAINTENANCE COEFFICIENTS = 0.0070
 PIPE LENGTH = 15.0000 M.

FLUM SUPERCRITICAL, NORMAL DEPTH = 0.0113 M. AND CRITICAL DEPTH = 0.0131 M.

INITIAL FLOW RATE = 0.2000 L/S. INITIAL DEPTH = 0.0113 M. INITIAL WAVE SPEED = 0.2747 M/S.

CALCULATION TIME STEP = 1.0935 S. LENGTH INCREMENT = 0.7500 M. NUMBER OF NODES = 21 IFAC = 1.00

H = 0.112610E+01 V = 0.411121E+00
 Q = 0.200000E+00 C = 0.274747E+00

TIME	S.	DEPTH	M/S	VELOCITY	M/S	FLOW RATE	L/S	WAVE SPD.	M/S	POSITION FROM ENTRY M.	0.	1.500	3.000	4.500	6.000	7.500	9.000	10.500	12.000	13.500	15.000	
0.	0.	0.0113	0.0113	0.4111	0.4111	0.2000	0.2000	0.2747	0.2747	0.0113	0.0113	0.0113	0.0113	0.0113	0.0113	0.0113	0.0113	0.0113	0.0113	0.0113	0.0113	0.0113
1.09	1.09	0.0113	0.0113	0.4111	0.4111	0.2000	0.2000	0.2747	0.2747	0.0113	0.0113	0.0113	0.0113	0.0113	0.0113	0.0113	0.0113	0.0113	0.0113	0.0113	0.0113	0.0113
2.19	2.19	0.0113	0.0113	0.4111	0.4111	0.2000	0.2000	0.2747	0.2747	0.0113	0.0113	0.0113	0.0113	0.0113	0.0113	0.0113	0.0113	0.0113	0.0113	0.0113	0.0113	0.0113
3.01	3.01	0.0113	0.0113	0.4111	0.4111	0.2000	0.2000	0.2747	0.2747	0.0113	0.0113	0.0113	0.0113	0.0113	0.0113	0.0113	0.0113	0.0113	0.0113	0.0113	0.0113	0.0113
3.72	3.72	0.0113	0.0113	0.4111	0.4111	0.2000	0.2000	0.2747	0.2747	0.0113	0.0113	0.0113	0.0113	0.0113	0.0113	0.0113	0.0113	0.0113	0.0113	0.0113	0.0113	0.0113
4.38	4.38	0.0113	0.0113	0.4111	0.4111	0.2000	0.2000	0.2747	0.2747	0.0113	0.0113	0.0113	0.0113	0.0113	0.0113	0.0113	0.0113	0.0113	0.0113	0.0113	0.0113	0.0113
5.01	5.01	0.0113	0.0113	0.4111	0.4111	0.2000	0.2000	0.2747	0.2747	0.0113	0.0113	0.0113	0.0113	0.0113	0.0113	0.0113	0.0113	0.0113	0.0113	0.0113	0.0113	0.0113
5.65	5.65	0.0113	0.0113	0.4111	0.4111	0.2000	0.2000	0.2747	0.2747	0.0113	0.0113	0.0113	0.0113	0.0113	0.0113	0.0113	0.0113	0.0113	0.0113	0.0113	0.0113	0.0113

TIME = 14.75 S.	M = 0.0113	0.0124	0.0172	0.0263	0.0254	0.0237	0.0205	0.0127	0.0113	0.0113
VELOCITY	M/S = 0.4111	0.4090	0.4906	0.6153	0.7020	0.6707	0.6601	0.6612	0.4114	0.4111
FLOW RATE	L/S = 0.2000	0.2415	0.4400	0.8255	1.1576	1.0199	0.7736	0.2679	0.2604	0.2600
WAVE SPD.	M/S = 0.2747	0.2947	0.3916	0.3903	0.4204	0.4076	0.1751	0.2925	0.2749	0.2747
TIME = 15.41 S.	M = 0.0113	0.0124	0.0156	0.0260	0.0257	0.0244	0.0220	0.0157	0.0114	0.0113
VELOCITY	M/S = 0.4111	0.4094	0.4607	0.5674	0.6064	0.7024	0.6986	0.5830	0.4142	0.4111
FLOW RATE	L/S = 0.2000	0.2771	0.3616	0.6797	1.0121	1.1229	1.0377	0.4736	0.2639	0.2600
WAVE SPD.	M/S = 0.2747	0.2949	0.3256	0.3757	0.4153	0.4118	0.3093	0.2267	0.2759	0.2747
TIME = 16.08 S.	M = 0.0113	0.0121	0.0146	0.0232	0.0260	0.0250	0.0230	0.0169	0.0119	0.0113
VELOCITY	M/S = 0.4111	0.4063	0.4417	0.5278	0.6270	0.6946	0.6897	0.6387	0.4316	0.4112
FLOW RATE	L/S = 0.2000	0.2143	0.3124	0.5360	0.8650	1.01394	1.0715	0.9432	0.6598	0.2601
WAVE SPD.	M/S = 0.2747	0.2845	0.3136	0.3574	0.4003	0.4260	0.4167	0.3591	0.3597	0.2822
TIME = 16.74 S.	M = 0.0113	0.0114	0.0138	0.0172	0.0214	0.0249	0.0230	0.0209	0.0137	0.0113
VELOCITY	M/S = 0.4111	0.4070	0.4306	0.4475	0.5884	0.6697	0.7000	0.6691	0.4941	0.4122
FLOW RATE	L/S = 0.2000	0.2126	0.2804	0.4464	0.7242	1.0169	1.0981	0.7963	0.3202	0.2614
WAVE SPD.	M/S = 0.2747	0.2817	0.3047	0.3422	0.3837	0.4153	0.4205	0.4066	0.3742	0.2752
TIME = 17.41 S.	M = 0.0113	0.0117	0.0132	0.0160	0.0198	0.0274	0.0257	0.0222	0.0169	0.0115
VELOCITY	M/S = 0.4111	0.4074	0.4229	0.4751	0.5539	0.6366	0.7002	0.6959	0.6812	0.5906
FLOW RATE	L/S = 0.2000	0.2088	0.2566	0.3864	0.6094	0.8494	1.1191	1.0378	0.8657	0.5195
WAVE SPD.	M/S = 0.2747	0.2783	0.2925	0.3196	0.3544	0.3891	0.4147	0.4170	0.4007	0.3664
TIME = 18.08 S.	M = 0.0113	0.0115	0.0127	0.0151	0.0194	0.0220	0.0240	0.0232	0.0196	0.0124
VELOCITY	M/S = 0.4111	0.4096	0.4195	0.4587	0.5256	0.6032	0.6719	0.6876	0.6478	0.4497
FLOW RATE	L/S = 0.2000	0.2061	0.2432	0.3418	0.5217	0.7708	1.0142	1.0706	0.9503	0.2716
WAVE SPD.	M/S = 0.2747	0.2783	0.2925	0.3196	0.3544	0.3891	0.4147	0.4170	0.4007	0.3664
TIME = 18.74 S.	M = 0.0113	0.0115	0.0124	0.0143	0.0172	0.0206	0.0234	0.0240	0.0213	0.0140
VELOCITY	M/S = 0.4111	0.4093	0.4157	0.4467	0.5028	0.5780	0.6496	0.6701	0.6504	0.5094
FLOW RATE	L/S = 0.2000	0.2043	0.2320	0.3090	0.4542	0.6669	0.9095	1.0966	1.0004	0.3829
WAVE SPD.	M/S = 0.2747	0.2772	0.2883	0.3112	0.3425	0.3758	0.4043	0.4207	0.4077	0.3164
TIME = 19.41 S.	M = 0.0113	0.0114	0.0121	0.0137	0.0163	0.0193	0.0224	0.0246	0.0225	0.0179
VELOCITY	M/S = 0.4111	0.4098	0.4140	0.4378	0.4947	0.5470	0.6140	0.6730	0.6941	0.6127
FLOW RATE	L/S = 0.2000	0.2030	0.2237	0.2844	0.4023	0.5820	0.8046	1.0106	1.0401	0.8986
WAVE SPD.	M/S = 0.2747	0.2765	0.2851	0.3043	0.3322	0.3636	0.3928	0.4132	0.3939	0.3495
TIME = 20.04 S.	M = 0.0113	0.0113	0.0119	0.0132	0.0154	0.0182	0.0211	0.0237	0.0234	0.0202
VELOCITY	M/S = 0.4111	0.4101	0.4128	0.4312	0.4702	0.5251	0.5873	0.6476	0.6957	0.6541
FLOW RATE	L/S = 0.2000	0.2020	0.2176	0.2655	0.3619	0.5134	0.7110	0.9197	1.0716	0.9580
WAVE SPD.	M/S = 0.2747	0.2760	0.2826	0.2965	0.3233	0.3525	0.3813	0.4049	0.4176	0.4023
TIME = 20.76 S.	M = 0.0113	0.0113	0.0117	0.0128	0.0147	0.0172	0.0200	0.0226	0.0244	0.0216
VELOCITY	M/S = 0.4111	0.4104	0.4124	0.4262	0.4547	0.5068	0.5622	0.6235	0.6903	0.6713
FLOW RATE	L/S = 0.2000	0.2014	0.2130	0.2509	0.3309	0.4579	0.6310	0.8255	1.0003	0.8901
WAVE SPD.	M/S = 0.2747	0.2756	0.2806	0.2916	0.3156	0.3425	0.3704	0.3952	0.4119	0.4084
TIME = 21.44 S.	M = 0.0113	0.0113	0.0116	0.0125	0.0141	0.0164	0.0190	0.0216	0.0247	0.0227
VELOCITY	M/S = 0.4111	0.4106	0.4117	0.4274	0.4493	0.4914	0.5481	0.6094	0.6509	0.6929
FLOW RATE	L/S = 0.2000	0.2010	0.2095	0.2393	0.3045	0.4129	0.5637	0.7446	0.9237	1.0434
WAVE SPD.	M/S = 0.2747	0.2753	0.2791	0.2899	0.3047	0.3337	0.3603	0.3843	0.4048	0.4140
TIME = 22.11 S.	M = 0.0113	0.0113	0.0115	0.0122	0.0136	0.0157	0.0181	0.0208	0.0242	0.0236
VELOCITY	M/S = 0.4111	0.4104	0.4114	0.4195	0.4417	0.4784	0.5291	0.5868	0.6203	0.6659
FLOW RATE	L/S = 0.2000	0.2007	0.2069	0.2303	0.2940	0.3759	0.5073	0.6870	0.9686	0.9686
WAVE SPD.	M/S = 0.2747	0.2751	0.2790	0.2907	0.3032	0.3257	0.3509	0.3766	0.3966	0.4098
TIME = 22.79 S.	M = 0.0113	0.0111	0.0115	0.0120	0.0132	0.0150	0.0172	0.0200	0.0218	0.0209
VELOCITY	M/S = 0.4111	0.4104	0.4114	0.4195	0.4417	0.4784	0.5291	0.5868	0.6203	0.6659
FLOW RATE	L/S = 0.2000	0.2007	0.2069	0.2303	0.2940	0.3759	0.5073	0.6870	0.9686	0.9686
WAVE SPD.	M/S = 0.2747	0.2751	0.2790	0.2907	0.3032	0.3257	0.3509	0.3766	0.3966	0.4098

TIME = 23.47 S.	FLUM RATE L/S= 0.2064	0.2050	0.2731	0.2673	0.3454	0.4578	0.4059	0.7699	0.4224	1.0133
	WAVE SPD. M/S= 0.2747	0.2750	0.2771	0.2791	0.3166	0.3424	0.3604	0.3880	0.4040	0.4461
	DEPTH M= 0.0113	0.0114	0.0118	0.0126	0.0144	0.0165	0.0185	0.0209	0.0228	0.0439
	VELOCITY M/S= 0.4111	0.4109	0.4111	0.4155	0.4303	0.4580	0.4961	0.5404	0.5872	0.6329
	FLUM RATE L/S= 0.2060	0.2001	0.2031	0.2177	0.2537	0.3201	0.4177	0.5501	0.7017	0.8543
	WAVE SPD. M/S= 0.2747	0.2749	0.2765	0.2740	0.3123	0.3345	0.3577	0.3795	0.3972	0.4072
TIME = 24.17 S.	FLUM RATE L/S= 0.0113	0.0114	0.0117	0.0125	0.0139	0.0174	0.0179	0.0201	0.0220	0.0434
	WAVE SPD. M/S= 0.4111	0.4110	0.4142	0.4261	0.4499	0.4840	0.5249	0.5691	0.6133	0.6540
	DEPTH M= 0.0113	0.0113	0.0113	0.0126	0.0140	0.0174	0.0179	0.0201	0.0220	0.0434
	VELOCITY M/S= 0.2000	0.2002	0.2133	0.2425	0.2986	0.3672	0.4512	0.6338	0.7871	0.9156
	FLUM RATE L/S= 0.2747	0.2749	0.2760	0.2903	0.3066	0.3272	0.3495	0.3711	0.3897	0.4027
TIME = 24.00 S.	FLUM RATE L/S= 0.0113	0.0113	0.0116	0.0123	0.0135	0.0152	0.0172	0.0192	0.0212	0.0428
	WAVE SPD. M/S= 0.4111	0.4110	0.4133	0.4226	0.4428	0.4713	0.5109	0.5523	0.5947	0.6353
	DEPTH M= 0.0113	0.0113	0.0113	0.0126	0.0140	0.0174	0.0179	0.0201	0.0220	0.0434
	VELOCITY M/S= 0.2000	0.2001	0.2099	0.2332	0.2592	0.3071	0.3542	0.4092	0.4582	0.5058
	FLUM RATE L/S= 0.2747	0.2748	0.2756	0.2749	0.3015	0.3204	0.3416	0.3628	0.3820	0.3969
TIME = 25.01 S.	FLUM RATE L/S= 0.0113	0.0113	0.0115	0.0121	0.0131	0.0146	0.0164	0.0194	0.0204	0.0421
	WAVE SPD. M/S= 0.4111	0.4110	0.4126	0.4198	0.4367	0.4637	0.4982	0.5369	0.5773	0.6170
	DEPTH M= 0.0113	0.0113	0.0113	0.0126	0.0140	0.0174	0.0179	0.0201	0.0220	0.0434
	VELOCITY M/S= 0.2000	0.2001	0.2073	0.2257	0.2648	0.3294	0.4203	0.5342	0.6636	0.7946
	FLUM RATE L/S= 0.2747	0.2748	0.2754	0.2779	0.2846	0.2967	0.3141	0.3341	0.3548	0.3741
TIME = 26.35 S.	FLUM RATE L/S= 0.0113	0.0113	0.0114	0.0119	0.0128	0.0141	0.0156	0.0177	0.0196	0.0413
	WAVE SPD. M/S= 0.4111	0.4111	0.4120	0.4175	0.4314	0.4551	0.4865	0.5227	0.5610	0.5994
	DEPTH M= 0.0113	0.0113	0.0113	0.0126	0.0140	0.0174	0.0179	0.0201	0.0220	0.0434
	VELOCITY M/S= 0.2000	0.2001	0.2057	0.2195	0.2516	0.3070	0.3869	0.4894	0.6098	0.7349
	FLUM RATE L/S= 0.2747	0.2748	0.2752	0.2770	0.2824	0.2929	0.3084	0.3271	0.3470	0.3662
TIME = 27.11 S.	FLUM RATE L/S= 0.0113	0.0113	0.0114	0.0117	0.0125	0.0136	0.0152	0.0170	0.0188	0.0406
	WAVE SPD. M/S= 0.4111	0.4111	0.4117	0.4157	0.4269	0.4474	0.4759	0.5095	0.5458	0.5827
	DEPTH M= 0.0113	0.0113	0.0113	0.0126	0.0140	0.0174	0.0179	0.0201	0.0220	0.0434
	VELOCITY M/S= 0.2000	0.2000	0.2037	0.2156	0.2407	0.2874	0.3593	0.4493	0.5587	0.6761
	FLUM RATE L/S= 0.2747	0.2748	0.2750	0.2764	0.2808	0.2894	0.3031	0.3205	0.3395	0.3550
TIME = 27.90 S.	FLUM RATE L/S= 0.0113	0.0113	0.0114	0.0118	0.0122	0.0132	0.0146	0.0163	0.0181	0.0498
	WAVE SPD. M/S= 0.4111	0.4111	0.4114	0.4143	0.4232	0.4407	0.4662	0.4973	0.5316	0.5669
	DEPTH M= 0.0113	0.0113	0.0113	0.0126	0.0140	0.0174	0.0179	0.0201	0.0220	0.0434
	VELOCITY M/S= 0.2000	0.2000	0.2026	0.2108	0.2315	0.2709	0.3317	0.4134	0.5131	0.6249
	FLUM RATE L/S= 0.2747	0.2748	0.2749	0.2759	0.2791	0.2863	0.2984	0.3143	0.3324	0.3509
TIME = 28.70 S.	FLUM RATE L/S= 0.0113	0.0113	0.0113	0.0115	0.0120	0.0129	0.0141	0.0156	0.0173	0.0490
	WAVE SPD. M/S= 0.4111	0.4111	0.4113	0.4133	0.4201	0.4347	0.4574	0.4861	0.5183	0.5520
	DEPTH M= 0.0113	0.0113	0.0113	0.0126	0.0140	0.0174	0.0179	0.0201	0.0220	0.0434
	VELOCITY M/S= 0.2000	0.2000	0.2018	0.2078	0.2241	0.2507	0.3040	0.3815	0.4718	0.5755
	FLUM RATE L/S= 0.2747	0.2748	0.2749	0.2756	0.2780	0.2838	0.2941	0.3086	0.3255	0.3409
TIME = 29.52 S.	FLUM RATE L/S= 0.0113	0.0113	0.0113	0.0114	0.0118	0.0125	0.0136	0.0152	0.0166	0.0483
	WAVE SPD. M/S= 0.4111	0.4111	0.4112	0.4125	0.4177	0.4244	0.4494	0.4756	0.5058	0.5360
	DEPTH M= 0.0113	0.0113	0.0113	0.0126	0.0140	0.0174	0.0179	0.0201	0.0220	0.0434
	VELOCITY M/S= 0.2000	0.2000	0.2012	0.2055	0.2181	0.2447	0.2930	0.3544	0.4300	0.5200
	FLUM RATE L/S= 0.2747	0.2748	0.2746	0.2753	0.2771	0.2817	0.2904	0.3033	0.3191	0.3363
TIME = 30.36 S.	FLUM RATE L/S= 0.0113	0.0113	0.0113	0.0114	0.0117	0.0123	0.0132	0.0145	0.0160	0.0476
	WAVE SPD. M/S= 0.4111	0.4111	0.4111	0.4120	0.4158	0.4253	0.4424	0.4669	0.4942	0.5247
	DEPTH M= 0.0113	0.0113	0.0113	0.0126	0.0140	0.0174	0.0179	0.0201	0.0220	0.0434
	VELOCITY M/S= 0.2000	0.2000	0.2004	0.2026	0.2108	0.2315	0.2709	0.3317	0.4134	0.5131
	FLUM RATE L/S= 0.2747	0.2747	0.2747	0.2748	0.2751	0.2754	0.2749	0.2747	0.2744	0.2742
TIME = 31.22 S.	FLUM RATE L/S= 0.0113	0.0113	0.0113	0.0114	0.0116	0.0120	0.0129	0.0149	0.0154	0.0469
	WAVE SPD. M/S= 0.4111	0.4111	0.4111	0.4115	0.4143	0.4218	0.4461	0.4727	0.4933	0.5122
	DEPTH M= 0.0113	0.0113	0.0113	0.0126	0.0140	0.0174	0.0179	0.0201	0.0220	0.0434
	VELOCITY M/S= 0.2000	0.2000	0.2001	0.2026	0.2107	0.2315	0.2709	0.3317	0.4134	0.5131
	FLUM RATE L/S= 0.2747	0.2747	0.2747	0.2748	0.2748	0.2748	0.2748	0.2748	0.2748	0.2748
TIME = 32.10 S.	FLUM RATE L/S= 0.0113	0.0113	0.0113	0.0113	0.0115	0.0119	0.0125	0.0136	0.0148	0.0463
	WAVE SPD. M/S= 0.4111	0.4111	0.4111	0.4114	0.4132	0.4199	0.4412	0.4642	0.4871	0.5063
	DEPTH M= 0.0113	0.0113	0.0113	0.0126	0.0140	0.0174	0.0179	0.0201	0.0220	0.0434
	VELOCITY M/S= 0.2000	0.2000	0.2001	0.2026	0.2107	0.2315	0.2709	0.3317	0.4134	0.5131
	FLUM RATE L/S= 0.2747	0.2747	0.2747	0.2748	0.2748	0.2748	0.2748	0.2748	0.2748	0.2748

U.S. DEPT. OF COMM. BIBLIOGRAPHIC DATA SHEET <i>(See instructions)</i>	1. PUBLICATION OR REPORT NO. NBSIR 82-2478	2. Performing Organ. Report No.	3. Publication Date March 1982
4. TITLE AND SUBTITLE Application of the Method of Characteristics to Predict Attenuation in Unsteady Partially-Filled Pipe Flow			
5. AUTHOR(S) John Swaffield			
6. PERFORMING ORGANIZATION <i>(If joint or other than NBS, see instructions)</i> NATIONAL BUREAU OF STANDARDS DEPARTMENT OF COMMERCE WASHINGTON, D.C. 20234		7. Contract/Grant No. H-48-78	8. Type of Report & Period Covered
5. SPONSORING ORGANIZATION NAME AND COMPLETE ADDRESS <i>(Street, City, State, ZIP)</i> Department of Housing and Urban Development 451 7th Street, SW Washington, DC 20410			
10. SUPPLEMENTARY NOTES <input type="checkbox"/> Document describes a computer program; SF-185, FIPS Software Summary, is attached.			
11. ABSTRACT <i>(A 200-word or less factual summary of most significant information. If document includes a significant bibliography or literature survey, mention it here)</i> The mechanism of flow attenuation in partially filled unsteady pipe flow is presented and shown to have relevance to the design of gravity drainage systems. The equations defining unsteady flow in partially filled pipe are derived and shown to be capable of solution by means of the method of characteristics. This technique as a method of predicting flow depth, velocity and wave speed along a long drainage pipe at a range of pipe gradients, diameters, and roughness coefficients was tested by means of numerical examples for a series of simulations run on a digital computer. Additionally, limited experimental verification of the analysis technique is presented for the supercritical flow response to a short duration inflow surge. Generally, the technique developed was found to be applicable to the design of drainage systems and further work is proposed to both extend the experimental verification and for the greater complexity of the multi-branched pipe system.			
12. KEY WORDS <i>(Six to twelve entries; alphabetical order; capitalize only proper names; and separate key words by semicolons)</i> building drainage; computer model; surge attenuation; unsteady flow.			
13. AVAILABILITY <input checked="" type="checkbox"/> Unlimited <input type="checkbox"/> For Official Distribution. Do Not Release to NTIS <input type="checkbox"/> Order From Superintendent of Documents, U.S. Government Printing Office, Washington, D.C. 20402. <input checked="" type="checkbox"/> Order From National Technical Information Service (NTIS), Springfield, VA. 22161		14. NO. OF PRINTED PAGES 88	15. Price \$10.50

